Arabian Journal of Geosciences (2022) 15: 39
https://doi.org/10.1007/s12517-021-08574-2

ORIGINAL PAPER

Geochemical characteristics and source of crude oil in the Shenhu uplift, Pearl River Mouth Basin, South China Sea

Xiaoyan Fu[1] · Shijia Chen[1] · Xin He[1] · Junjun You[2] · Hui Li[2] · Mingzhu Lei[2]

Received: 4 June 2021 / Accepted: 5 October 2021 / Published online: 27 December 2021
© Saudi Society for Geosciences 2021

Abstract

There is a lack of systematic study on geochemical characteristics and the source of crude oil in Shenhu uplift area of the Pearl River Mouth Basin (PRMB). Under such circumstances, the Rock–Eval, gas chromatography (GC), and gas chromatography-mass spectrometry (GC–MS) experiments were carried out. The results show that the following: (1) The medium-deep lacustrine source rocks of the Wenchang Formation (MWC) in the Wenchang-B depression have the highest organic matter abundance. The shallow lacustrine source rocks of the Wenchang Formation (SWC) in Wenchang-B depression and the shallow lacustrine source rocks of the Enping Formation (SEP) in the Wenchang-A depression have relatively low organic matter abundance, but three sets of hydrocarbons have reached the mature stage and have good hydrocarbon generation potential. (2) The *n*-alkanes of crude oil in the Shenhu uplift have pre-peak characteristics, and the Pr/Ph > 2.00. The tricyclic terpene (TT) content is relatively low, and C_{19}-C_{20}-C_{21}-C_{23}TT presents a "low–high-low" distribution characteristic. Meanwhile, the content of rearranged sesquiterpanes is higher in bicyclic sesquiterpanes. In addition, ααα20RC_{27}-ααα20RC_{28}-ααα20RC_{29} regular steranes are "L"-shaped, C_{30}-4 methyl sterane (C_{30}-4MSt)/C_{29} regular sterane values are between 0.24 and 0.34, and dicadinane (W + T)/C_{30}H values are 1.08–1.61. By comparing these biomarkers with source rocks one by one, it is finally found that the crude oil has the closest genetic relationship with the SEP in well WA4.

Keywords Pearl River Mouth Basin · Shenhu uplift · Geochemical characteristics · Oil source relations · Zhu-3 sub-basin

Introduction

The crude oil geochemical characteristics and the oil-source correlation are critical in determining the type of crude oil, clarifying the oil and gas system, and studying the law of oil and gas accumulation (Hao et al. 2011; Huang et al. 2011; Aldahik et al. 2017). Molecular geochemistry has been widely used since the 1970s (Rubinstein et al. 1979; Brooks and Thusu 1977). This method still has a reliable application value (Luo et al. 2020; Wang and Guo 2020).

The Shenhu uplift is located in the western part of the Pearl River Mouth Basin (PRMB) (Fig. 1a). Since drilling in 2001, high oil flows have been obtained from the Neogene Miocene Zhujiang Formation (Chen et al. 2015). There are no tertiary strata in the Shenhu uplift area, so there is a lack of Wenchang and Enping Formation. Therefore, the oil source in this area comes from the Zhu-3 depression, which is closer to the area (Quan et al. 2015; Fu et al. 2011) (Fig. 1a). There are three sedimentary centers in Zhu-3 sub-basin, namely Wenchang-A depression, Wenchang-B depression, and Wenchang-C depression (Fig. 1b). However, no source rock was found in Wenchang-C depression.

After years of oil–gas exploration, predecessors had done many studies on the source rock characteristics of Wenchang-A depression and Wenchang-B depression in Zhu-3 sub-basin (Huang et al. 2003; Cheng et al. 2015), which provided a great reference value for the oil source research in the Shenhu uplift area. The characteristics and sources of crude oil around the Zhu-3 depression have also been the focus of researchers for many years (Zhou and Zhang 2000; Xiao et al. 2009). But as far as the Shenhu uplift area is concerned, previous studies mainly focused on the tectonic evolution, sequence stratigraphy, and sedimentary evolution

Responsible Editor: Santanu Banerjee.

✉ Shijia Chen
chensj1964@sina.cn

[1] School of Geoscience and Technology, Southwest Petroleum University, Sichuan Province, Chengdu, China

[2] Hainan Branch of China National Offshore Oil Corporation Ltd, Hainan, China

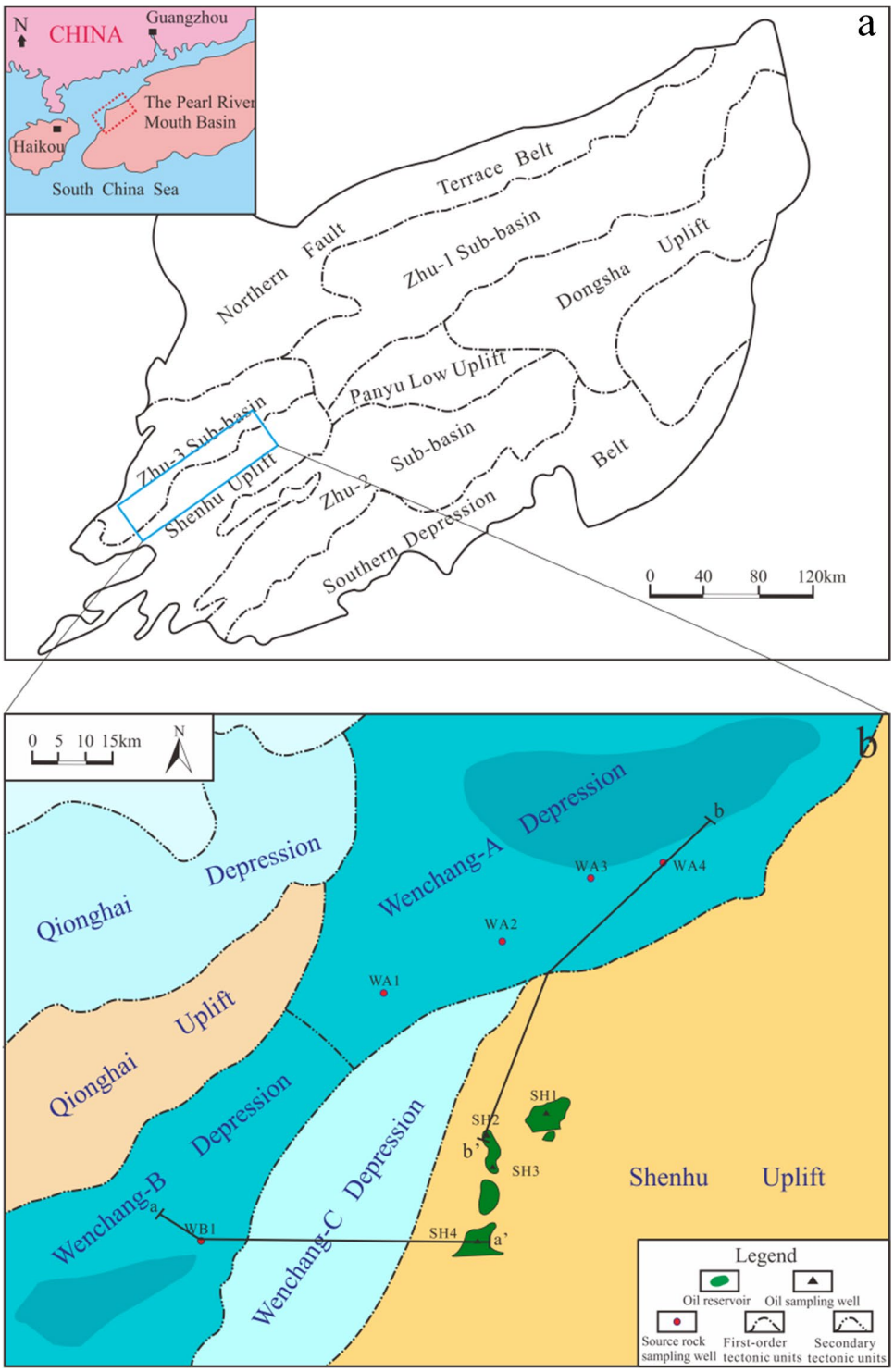

Fig. 1 Sub-basins of Pearl River Mouth Basin, China (a, modified from Hu et al. 2015). Reservoir distribution in Shenhu uplift area and source rock distribution in Zhu-3 sub-basin (b, modified from Fu et al. 2011)

(Xia et al. 1994; Wu et al. 2014). The oil source research of SH1 well reservoir also has a preliminary understanding (Chen et al. 2015; Quan et al. 2015). But there is still a lack of systematic research on the geochemical characteristics and oil source understanding of crude oil in the whole area, which restricts further exploration and deployment. Therefore, under the premise of discovering small oil reservoirs in the Shenhu uplift, what are the geochemical characteristics of the crude oil? The source rock layers of the adjacent Wenchang-A and Wenchang-B depressions are also different. What are the characteristics of these source rocks? Does it have good hydrocarbon generation potential? With multiple sets of source rocks, where does the crude oil come from? Is it from multiple sources or from a specific set

of source rocks? Clarifying these issues can provide a basis for future exploration and development and the study of the entire region. This study also can provide a reference value for exploring the areas lacking source rock development around major depressions in the PRMB, clarifying their oil sources and implementing further exploration.

Geological settings

The PRMB is a large sedimentary basin dominated by the Cenozoic on the continental shelf and slope of the northern South China Sea (Wu 1984). The basin is a typical passive margin Cenozoic rift basin formed on the pre Tertiary basement (Jiang et al. 2009). The basin can be divided into eight tectonic units, namely the Zhu-1, Zhu-2, and Zhu-3 sub-basins, Shenhu, Panyu low and Dongsha uplift, and Southern Depression Belt and Northern Fault zone, where the Shenhu uplift is located on the southern side of the Zhu-3 sub-basin (Fig. 1a).

The PRMB had experienced three major tectonic evolution stages since Cenozoic: syn-rifting stage, fault depression stage, and depression stage (Xu and Huang 2000; Hu et al., 2014) (Fig. 2). During the Eocene rifting period, the tectonic stress in the western part of the PRMB was mainly NW–SE extension, forming a NE-SW-trending depression-controlling southern fault of the Zhu-3 sub-basin. The strong rifting effect of this fault expanded the range of lake water in Wenchang-B depression, deepened the water sharply, formed lacustrine deposits, and developed thick Wenchang Formation mudstone (the strata between T90 and T80 reflection surfaces on the seismic reflection profile). After the Wenchang period, the area of strong fault activity moved eastward, resulting in the development of thick mudstone in the Enping Formation of the Wenchang-A depression (Zhu et al. 1997; Fu et al. 2011) (the layer between the T80-T70 reflecting surfaces on the seismic reflection profile) (Fig. 2). The influence of this fault caused the difference in source rocks between Wenchang-A depression and Wenchang-B depression in Zhu-3 sub-basin. During the fault deposition period, the Zhuhai Formation and Zhujiang Formation mainly composed of sand were developed. However, due to the influence of the southern Zhu-3 sub-basin fault, there was no Tertiary deposition in the Shenhu uplift. The Zhujiang Formation was directly connected to the bottom of the Pre-Triassic. The Zhujiang Formation became the reservoir in the area (the stratum between T60 and T40 reflection planes on the seismic reflection profile). The upper Hanjiang Formation (between T40 and T20 reflection planes on seismic reflection profile) deposited thick mudstones and fine sandstone due to the weakening of tectonic activity at that time, and became regional cap rocks.

Sample collection and experiments

Thirty samples were collected in this study, including 6 crude oil samples, 8 mudstone samples of Enping Formation in Wenchang-A depression, and 16 mudstone samples of Wenchang Formation in Wenchang-B depression. The pyrolysis, macerals of the mudstone samples were analyzed. In addition, all samples were analyzed by GC and GC–MS. Several Chinese industries or national standards (numbers prefixed with "SY/T" or "GB/T") are cited below, and these methods have been published publicly.

Pretreatment and Rock–Eval

According to GB/T19144-2010 standard, the samples were subjected to pre-pyrolysis treatment. The carbonates and silicates contained in the samples were removed by stepwise pickling (Xiao et al. 2021). The remaining water was dried with filter paper and the mudstone samples were crushed through mudstone crushing prototype machine, model MZ-100 (550×540×750), to make the particle size between 0.07 mm and 0.15 mm. The pyrolysis experiment of source rock was carried out according to GB/T 18,602–2012. The mudstone photo and rock composition were provided by CNOOC Zhanjiang Branch.

Determination of total organic carbon

First grind the sample to a particle size of less than 0.2 mm, weigh 0.01–1.00 g sample (required to be accurate to 0.0001 g), then slowly add excess hydrochloric acid solution, place it on a water bath or electric hot plate, and control the temperature at 60–80 °C for more than 2 h until the reaction is complete. Place the dissolved sample in the porcelain crucible of the suction filter and wash it with distilled water. Then, put the washed sample into an oven at 60–80 °C for drying. Finally, the Lcco CS-400 analyzer (600,191) was used to determine the total organic carbon in the sedimentary rock in the rock according to the GB/T 19,145–2003 standard.

GC and GC–MS experiments

The samples can be desorbed from the thermally evaporated hydrocarbon and the pyrolytic hydrocarbon respectively at different temperatures and constant temperatures controlled by the pyrolysis furnace. Both were carried by inert gas and separated into various monomer hydrocarbons and monomer compounds by capillary column chromatography, and detected by a flame-ion-detector. Refer to SY/T 6188–1996 industry standards. GC was carried out using a

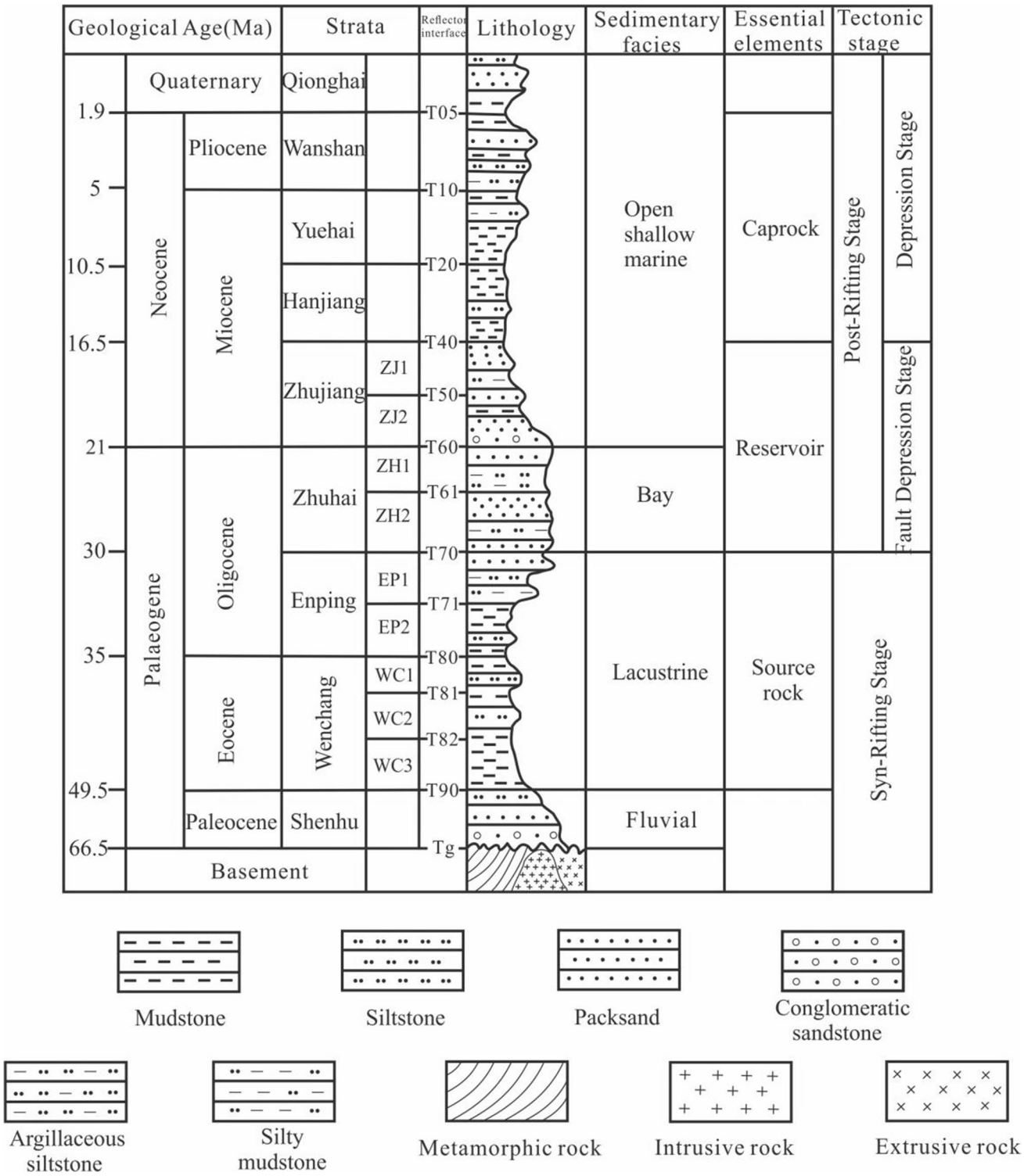

Fig. 2 Synthetic columnar profile of Zhu-3 sub-basin in Pearl River Mouth Basin. (modified from Cheng et al. 2015)

Trace instrument equipped with a TG-5MS (both Thermo Scientific) fused silica capillary column (30 m × 0.25 mm id, 0.25 mm film thickness); the initial temperature of the column temperature is not more than 50 ℃. And then program the temperature to 320 °C at 3 ~ 12 °C/min and keep the temperature constant for 15 min. Compounds were relatively quantified by integral areas of their peaks in the chromatogram.

All the samples used chloroform as the solvent, and the Soxhlet extraction method was used to extract the soluble organic bitumen in the experimental samples. After using *n*-hexane to remove the asphaltenes, silica gel-alumina (3:2) chromatography is used to separate saturated hydrocarbons, aromatic hydrocarbons, and non-hydrocarbons. According to SY 5258–1991, the saturated hydrocarbon fractions were analyzed using HP5890-5972 chromatography/mass spectrometry analyzer. A 60.00 m × 0.32 mm × 0.25 μm capillary column was configured. The initial temperature of heating was 100 °C, and the carrier gas was helium. The constant current mode was adopted. The ion source temperature was 230 °C, and the inlet temperature was set to 310 °C (Su et al. 2021).

Results and discussion

Basic geochemical characteristics of source rocks

Mudstone refers to the weakly consolidated clay that undergoes moderate metagenesis (such as squeezing, dehydration, recrystallization, and cementation) to form a strongly consolidated rock. When it is rich in certain organic matter and can generate oil and gas, it is called source rock (Tissot and Welte 1978). The study area is black mudstone (Fig. 3), and most of the components observed under the microscope are argillaceous (Fig. 4), with a small amount of quartz (Table 1).

Relevant data are shown in Table 2.

According to the existing production data and experimental methods, the source rock hydrocarbon supply horizon of Wenchang-A depression and Wenchang-B depression has been in dispute (Lin and Sun 1999; Xie et al. 2012). However, researchers generally believe that in order to provide hydrocarbon for reservoirs with a certain distance from the center of the depression, it is still dominated by medium-deep lake facies source rocks of Wenchang Formation (MWC), shallow lake facies source rocks of Wenchang Formation (SWC) in Wenchang-B depression, and shallow lacustrine source rocks of Enping Formation (SEP) in Wenchang-A depression (Zhu et al. 1999; Kang and Feng 2011). The distribution of MWC and SWC source rocks in Wenchang-B depression was concentrated, and for the SEP source rock in Wenchang-A depression, it was widely distributed. To accurately determine the oil source, four wells with different distances from the Wenchang-A deposition center were selected for discussion.

According to the pyrolysis data, the free hydrocarbon (S_1) content of the MWC is between 1.09 and 2.58 mg HC/g rock, and the pyrolysis hydrocarbon yield (S_2) is 5.14 ~ 19.92 mg HC/g rock. The source rocks have hydrocarbon generation potential ($S_1 + S_2$) is between 6.23 and 22.50 mg HC/g rock, the production index (PI) is 0.10 ~ 0.17, and the temperature with maximum hydrocarbon generation (Tmax) is 442 ~ 444 ℃, there is little difference between the various values. The PI of SWC is between 0.19 and 0.54, and the Tmax is 432 ~ 443 ℃. The PI of SEP is 0.10 ~ 0.41, and the Tmax is 435 ~ 485 ℃.

Through the intersection of PI and Tmax (Fig. 5a), it can be clearly seen that the two sets of source rock data of the Wenchang Formation are concentrated, except for the individual data of SWC, which are all distributed in the mature interval and have high hydrocarbon generation capacity (Peters and Moldowan 1994; Varma et al. 2019). The source rock data of the Enping Formation are scattered and have reached the mature stage, but the maturity is different. This may be related to the difference in sedimentary organic matter and environment in different areas of Wenchang-A depression (Biswas et al. 2020; Su et al. 2021). The total organic carbon (TOC) of the source rocks in the study area is between 0.75 and 4.75. On the S_2-TOC intersection chart (Fig. 5b), except for a sample parameter of well WA2 in the Fair area, all other parameters are good or excellent, indicating that the source rocks have high abundance of organic matter and great hydrocarbon generation potential (Tissot and Welte 1984; Hakimi et al. 2013).

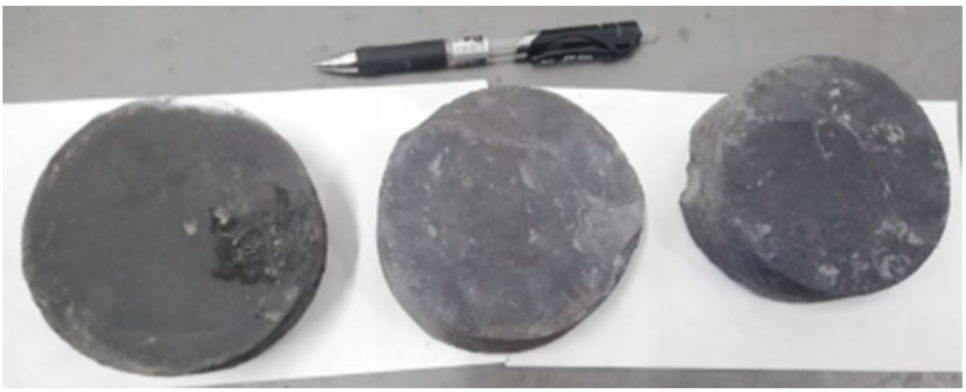

Fig. 3 Mudstone samples, left: WB1, WC2, 3234m; middle: WB1, WC1, 3019m; right: WA4, EP, 4122m

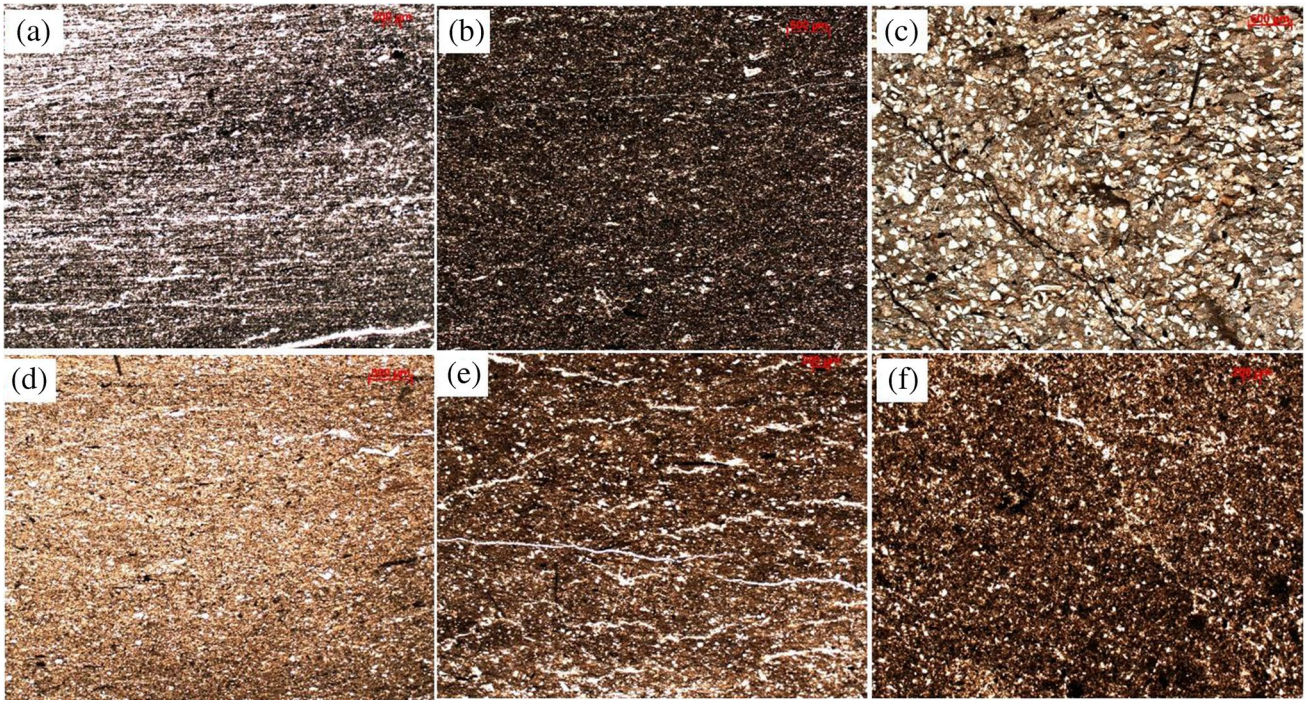

Fig. 4 Microscopic features of mudstone thin slices under single polarizer. Note: (a): WB1, WC2, 3234m; (b): WB1, WC1,3019m; (c): WA1, EP, 3391.83m; (d) WA2, EP, 3538m; (e) WA3, EP, 4507.55m; (f) WA4, EP, 4122m. Photo from CNOOC Zhanjiang Branch

Molecular geochemical characteristics of crude oil and source rocks

Characteristics of n-alkanes and isoprene

Relevant data are shown in Table 3.

Biomarker compounds retain various information such as the source of organic matter, deposition environment and maturity and have important applications for determining the oil-source correlation (Mackenzie 1984; Ahmed et al. 2020). *N*-alkanes and isoprene are rich in geological information. They are less affected by geological processes, thus widely used in studying molecular geochemical characteristics of crude oil and source rocks (Hunt 1979; Schwark and Frimmel 2004;).

N-alkanes can be divided into three parts—short-chain length *n*-alkanes (SCLAs: C_{14}–C_{20}), intermediate-chain length *n*-alkanes (ICLAs: C_{21}–C_{26}), and long-chain length *n*-alkanes (LCLAs: C_{27}–C_{31}) (Fig. 6). The *n*-alkanes of the crude oil in the study area are mainly SCLAs, and the content is between 0.44 and 0.55, indicating that the source of organic matter is mainly algae or microorganisms (Mayers and Ishiwatari 1995). Among them, the main peak carbon of SH1 well is nC_{20}, which indicates that this well may be a major contribution to bacterial lipids (Elias et al. 1997). The remaining four wells have nC_{17} as the main peak, indicating that the source is mainly algae lipids (Resmi et al. 2016). There are differences in the *n*-alkanes of different source rocks. It is particularly noted that the SCLAs in Well WA4 is relatively high, with nC_{17} and nC_{18} as the main sources, indicating that the source of organic matter is mainly algal lipids (Mayers and Ishiwatari 1995; Resmi et al. 2016), which is similar to the crude oil in the study area. The source rocks of other wells are mainly ICLAs. Ortiz et al. (2011) believed that nC_{21}-nC_{23} mainly came from ferns, and Bechtel et al. (2018) reported that nC_{27} and nC_{28} mainly represented terrestrial woody plants. It shows that the organic matter of the remaining source rocks not only contributes to ferns but also comes from terrestrial woody plants. The LCLA distribution of crude oil and source rocks has nothing to do with carbon preference index (CPI, related to LCLAs) and odd–even predominance (OEP, related to LCLAs), which may additionally indicate that the contribution of terrestrial plant-derived organic matter is negligible (Tiwari et al. 2020). Therefore, the CPI value may indicate the input of organic matter from aquatic plants (Punyu et al. 2013).

Due to the presence of wax on the surface of plants, the lipids of aquatic plants and terrestrial plants are similar (Aichner et al. 2010). Therefore, in order to distinguish the types of the source plants that provide lipids, Ficken et al. (2000) introduced a proxy ratio P_{aq} (a ratio of intermediate chain length normal alkanes to longer chain length homologs). The P_{aq} parameter and the average chain length (ACL) value (another agent for determining the source

Table 1 Rock–Eval data of source rocks in the Zhu-3 sub-basin

Well	Source rock type	Depth	S_1 (mg HC/g rock)	S_2 (mg HC/g rock)	S_1+S_2 (mg HC/g rock)	Tmax (℃)	TOC (wt.%)	PI
WA1	SEP	3329	0.03	0.26	0.29	436	1.21	0.10
WA1	SEP	3391.83	0.05	0.34	0.39	435	1.05	0.13
WA2	SEP	3538	1.69	5.23	6.92	442	1.88	0.24
WA2	SEP	3632	0.27	1.45	1.72	441	0.75	0.16
WA3	SEP	4507.55	0.07	0.13	0.20	485	1.12	0.35
WA3	SEP	4512.15	0.05	0.17	0.22	476	1.42	0.23
WA4	SEP	4122	0.42	1.10	1.52	437	2.24	0.28
WA4	SEP	4380	0.48	0.69	1.17	467	1.64	0.41
WB1	SWC	2911	0.48	1.55	2.03	437	2.30	0.24
WB1	SWC	2963	0.41	0.61	1.02	436	2.98	0.40
WB1	SWC	2980	0.54	0.72	1.26	436	1.81	0.43
WB1	SWC	3019	0.61	0.51	1.12	437	2.06	0.54
WB1	SWC	3063	0.43	0.48	0.91	438	2.25	0.47
WB1	SWC	3080	0.46	0.62	1.08	439	3.58	0.43
WB1	SWC	3090	2.18	9.23	11.41	432	4.75	0.19
WB1	SWC	3149	0.49	0.44	0.93	443	3.04	0.53
WB1	MWC	3234	1.09	5.14	6.23	442	3.14	0.17
WB1	MWC	3250	1.82	17.31	19.13	442	4.19	0.10
WB1	MWC	3268	1.54	14.18	15.72	444	2.68	0.10
WB1	MWC	3300	2.25	16.32	18.57	440	2.32	0.12
WB1	MWC	3326	1.84	15.46	17.30	444	3.25	0.11
WB1	MWC	3346	2.03	16.06	18.09	442	2.32	0.11
WB1	MWC	3366	2.44	17.25	19.69	440	2.59	0.12
WB1	MWC	3400	2.58	19.92	22.50	442	2.03	0.11

S_1 = free hydrocarbons (mg HC/g rock); S_2 = pyrolytic hydrocarbon yield (mg HC/g rock); TOC = total organic carbon (wt.%); Tmax = temperature with maximum hydrocarbon generation (°C); PI: production index = $S_1/(S_1+S_2)$; SEP: shallow lake facies in the Enping Formation; SWC: shallow lake facies in the Wenchang Formation; MWC: medium-deep lake facies in the Wenchang Formation

of LCLAs) shows a strong negative linear correlation ($r = -0.91$, Fig. 7a), indicating that the main contribution of organic matter is not terrestrial plants. In addition, this parameter has a good positive correlation with SCLAs (Fig. 7b), which may further indicate that SCLAs come from aquatic plants.

The pristine (Pr) and phytane (Ph) in sediments are derived from chlorophyll's phytic alcohol side chain. The pristane is formed under oxygen condition, and the phytane is formed under reduction conditions. Therefore, they can indicate the environment of organic matter deposition (Seifert and Moldowan 1978; Patra et al. 2018; Samad et al. 2020). The Pr/Ph ratio of crude oil in the Shenhu uplift is between 2.35 and 3.28, indicating a weakly oxidized sedimentary environment, which is similar to the source rocks of MWC (Pr/Ph:2.31 ~ 2.64), well WA2 (Pr/Ph = 2.49)), and well WA4 (Pr/Ph = 2.59) environment. The information reflected by *n*-alkanes is as follows: the crude oil in the study area and the two sets of source rocks of the Wenchang Formation are quite different, while Pr/Ph shows that the crude oil environment in the Shenhu uplift area is similar to that of the MWC. The Pr/Ph is different from the information reflected by *n*-alkanes. Therefore, to determine the source of crude oil from the Shenhu uplift more accurately, it is necessary to refer to other biomarker compounds and apply multiple parameters to determine the source rock in the study area.

Characteristics of tricyclic terpenes and bicyclic sesquiterpenes

The full name of the peak in the mass spectrometer-chromatogram is shown in Table 4. Relevant parameters are shown in Table 5.

Because of their own characteristics, terpenoids have important applications in the comparative study of oil sources. This study highlights the relationship between tricyclic terpenes (TTs) and bicyclic sesquiterpenes in crude oil and source rocks. Tricyclic terpanes are considered as substitutes for sterols in the prokaryotic cell membrane

Table 2 Basic geochemical data of source rocks in the Zhu-3 sub-basin

Well	Source rock type	Depth	Sapropel(%)	Exinite(%)	Vitrinite(%)	Inertinite(%)	TI	Organic matter type
WA1	SEP	3329	60.3	0	31.8	7.9	28.6	II_2
WA1	SEP	3391.83	18.0	1.0	37.0	44.0	-53.3	III
WA2	SEP	3538	54.3	0.3	42.1	3.3	19.6	II_2
WA2	SEP	3632	16.8	0.6	63.3	19.3	-49.7	III
WA3	SEP	4507.55	27.1	0.3	54.2	18.4	-31.8	III
WA3	SEP	4512.15	79.0	0.0	13.0	8.0	61.3	II_1
WA4	SEP	4122	37.9	0.0	62.1	0.0	-8.7	III
WA4	SEP	4380	47.3	0.0	50.9	1.8	7.3	II_2
WB1	SWC	2911	68.0	2.0	23.5	6.5	44.9	II_1
WB1	SWC	2963	47.4	0.0	45.8	6.8	6.3	II_2
WB1	SWC	2980	52.8	0.9	43.3	3.0	17.8	II_2
WB1	SWC	3019	74.0	4.5	21.0	0.5	60.0	II_1
WB1	SWC	3063	54.0	1.0	44.0	1.0	20.5	II_2
WB1	SWC	3080	79.7	4.5	14.7	1.1	69.8	II_1
WB1	SWC	3090	75.3	6.7	8.0	10.0	62.7	II_1
WB1	SWC	3149	64.3	1.4	24.0	10.3	36.7	II_2
WB1	MWC	3234	90.0	4.0	6.0	0.0	87.5	I
WB1	MWC	3250	87.9	2.3	8.7	1.1	81.4	I
WB1	MWC	3268	74.0	4.5	21.0	0.5	60.0	II_1
WB1	MWC	3300	72.0	1.8	24.7	1.5	52.9	II_1
WB1	MWC	3326	71.4	2.0	22.3	4.3	51.4	II_1
WB1	MWC	3346	82.0	8.0	3.0	7.0	76.8	II_1
WB1	MWC	3366	86.6	9.0	4.0	0.4	87.7	I
WB1	MWC	3400	90.0	4.0	6.0	0.0	87.5	I

TI = (sapropel × 100 + exinite × 50 − vitrinite × 75 − inertinite × 100)/100

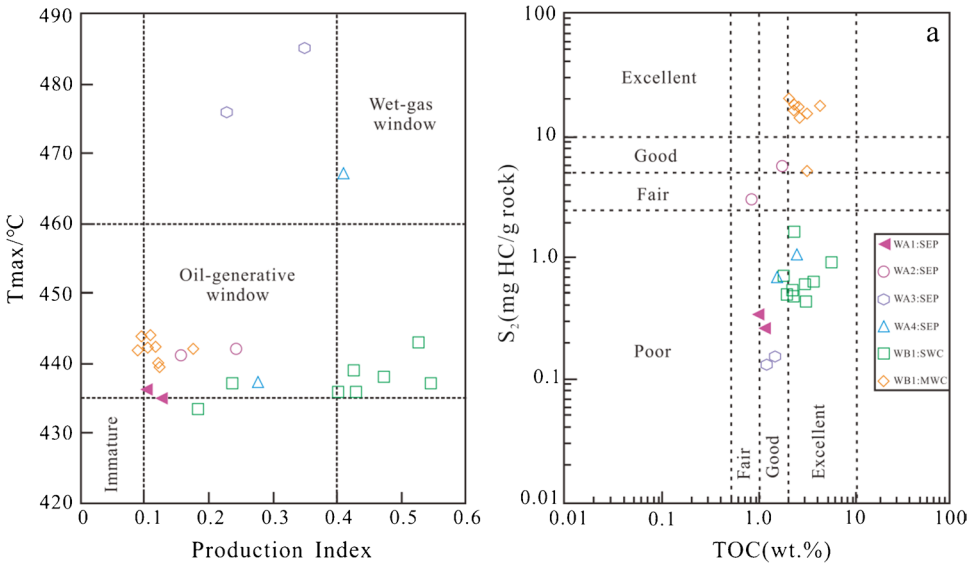

Fig. 5 Evaluation cross-plots of source rocks (**a**, Peters and Moldowan 1994; **b**, Tissot and Welte 1984; Su et al. 2021)

Table 3 Saturated hydrocarbon related parameters of crude oil and source rock

Well	Formation	Depth (m)	Main peak carbon	1	2	3	4	5	6	7	8	9	10	Sample type
WA1	EP	3391.83	nC_{28}	0.22	0.43	0.35	1.58	1.09	27.86	0.51	0.88	0.33	0.24	SEP
WA2	EP	3538	nC_{23}	0.27	0.49	0.24	1.63	1.11	27.08	0.64	2.49	2.15	0.54	
WA3	EP	4507.55	nC_{21}	0.27	0.47	0.26	1.56	1.10	27.61	0.57	1.08	0.69	0.45	
WA3	EP	4512.15	nC_{21}	0.26	0.47	0.27	1.55	1.09	27.59	0.58	0.97	0.78	0.27	
WA4	EP	4122	nC_{17}	0.43	0.42	0.15	1.54	1.01	26.57	0.72	2.59	0.44	0.17	
WA4	EP	4380	nC_{18}	0.43	0.41	0.16	1.53	1.02	26.58	0.71	1.85	0.30	0.16	
WB1	WC1	3019	nC_{21},nC_{27}	0.22	0.47	0.31	1.77	1.21	27.65	0.55	1.74	1.06	0.31	SWC
WB1	WC1	3149	nC_{20},nC_{27}	0.21	0.48	0.31	1.71	1.22	27.66	0.54	1.36	0.40	0.36	
WB1	WC2	3234	nC_{20},nC_{25}	0.22	0.46	0.32	1.69	1.14	27.58	0.53	2.64	0.34	0.13	MWC
WB1	WC2	3268	nC_{20},nC_{27}	0.35	0.39	0.26	1.67	1.13	27.59	0.56	2.31	0.33	0.14	
SH1	ZJ1	1269.6	nC_{20}	0.44	0.34	0.22	1.47	1.05	27.41	0.61	2.35	0.47	0.21	Oil
SH2	ZJ1	1205	nC_{17}	0.49	0.35	0.15	1.55	1.11	27.25	0.65	3.28	0.38	0.13	
SH3	ZJ1	1224	nC_{17}	0.55	0.32	0.14	1.59	1.11	27.27	0.65	3.21	0.37	0.13	
SH4	ZJ1	1143.5	nC_{17}	0.49	0.34	0.17	1.57	1.07	27.37	0.61	2.83	0.56	0.22	
SH4	ZJ1	1144.1	nC_{17}	0.51	0.34	0.15	1.58	1.08	27.36	0.62	2.90	0.32	0.11	
SH4	ZJ1	1145.8	nC_{17}	0.48	0.35	0.17	1.57	1.09	27.28	0.63	2.71	0.60	0.21	

1: short-chain length *n*-alkanes (SCLAs: C_{14}–C_{20}); 2: intermediate-chain length *n*-alkanes (ICLAs: C_{21}–C_{26}); 3: long-chain length *n*-alkanes (LCLAs: C_{27}–C_{31}); 4: odd–even predominance (OEP) = $(nC_{25}+6*\ nC_{27}+nC_{29})/(4*(nC_{26}+nC_{28}))$ (Tewari et al. 2017); 5: carbon preference index (CPI) = $(\ (nC_{23}+nC_{25}+nC_{27}+nC_{29}+nC_{31})+(\ nC_{25}+nC_{27}+nC_{29}+nC_{31}+nC_{33}))/(2*\ (nC_{24}+nC_{26}+nC_{28}+nC_{30}+nC_{32}))$ (El-Nemr et al. 2016); 6: average chain length (ACL) = $(25*\ nC_{25}+27*\ nC_{27}+29*nC_{29}+31*nC_{31}+33*nC_{33})/(nC_{25}+nC_{27}+nC_{29}+nC_{31}+nC_{33})$ (Ahmed et al. 2017) 7: proxy ratio (P_{aq}) = $(nC_{23}+nC_{25})/(nC_{23}+nC_{25}+nC_{27}+nC_{31})$ (Ficken et al. 2000); 8: Pristine (Pr)/ Phytane (Ph); 9: Pr/nC_{17};10: Ph/nC_{18}

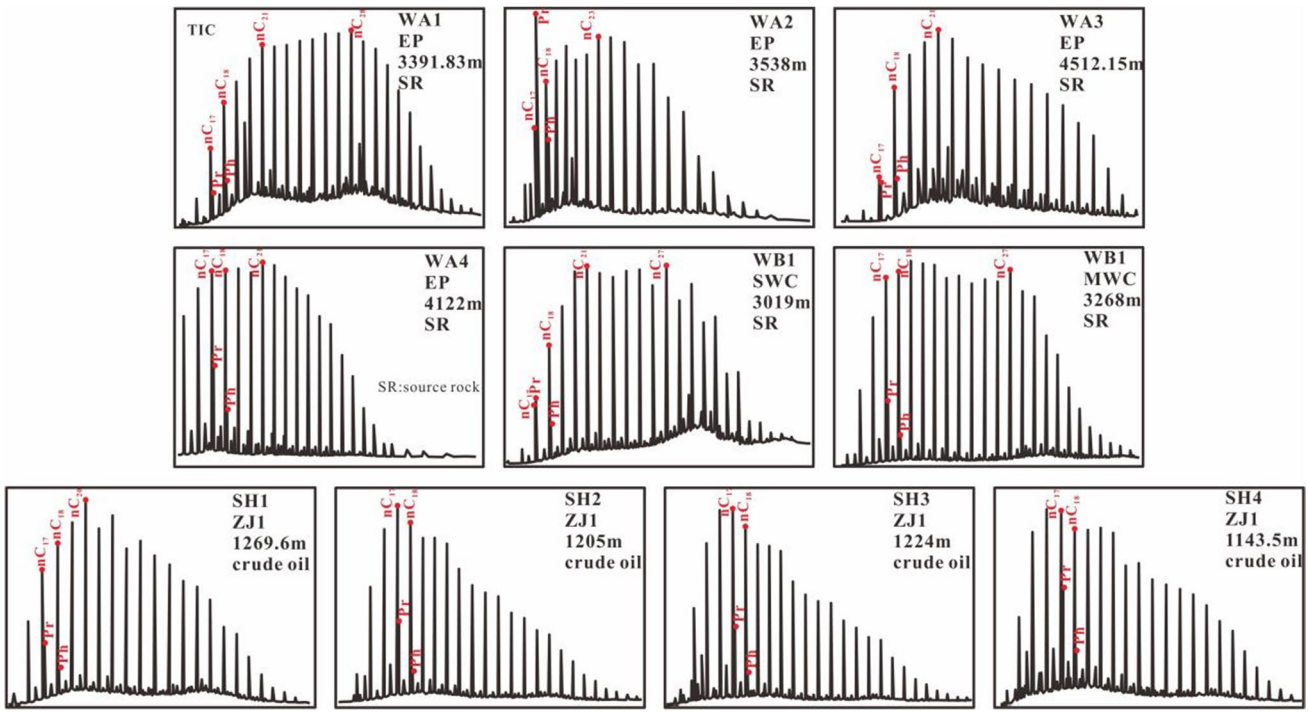

Fig. 6 Saturated hydrocarbon chromatogram of crude oil and source rocks

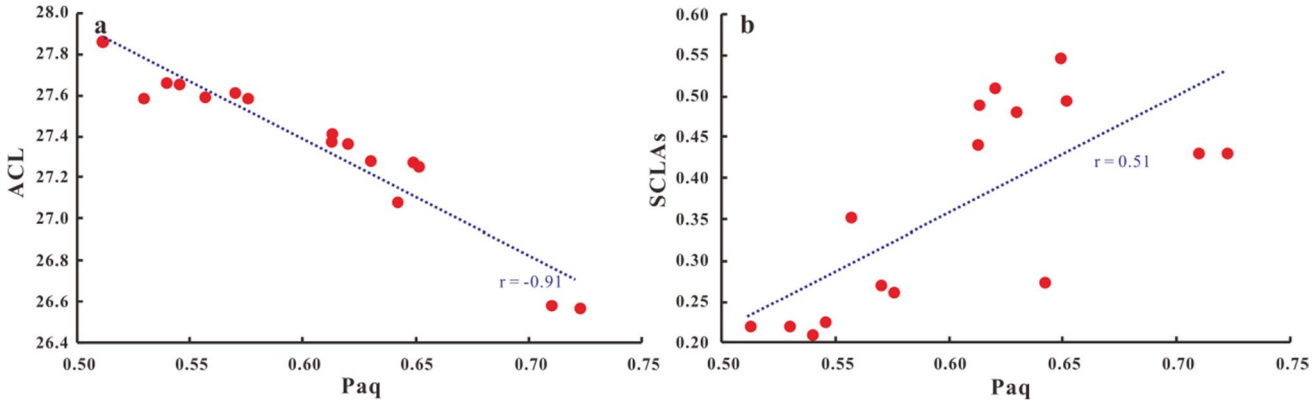

Fig. 7 Relation of proxy ratio (Paq) with average chain length (ACL) (**a**) and concentrations of short-chain length *n*-alkanes (SCLAs) (**b**)

(Neto et al. 1982; Grande et al. 1993), indicating the contribution of algae and microorganisms (Ourisson et al. 1982); Samuel et al. 2010). Previous studies found that the change of C_{19}–C_{23} TT could reflect the sedimentary environment and parent material source (Simoneit et al. 1990; Tao et al. 2015). The drimane series compounds in dicyclic sesquiterpenes are derived from bacteria and other microorganisms (Stout et al. 2005). They are formed by the reduction or rearrangement of degradation products of hopane precursors in the early stages of diagenesis. It is mainly related to the catalytic rearrangement of clay minerals in source rocks, that is, related to the sedimentary environment (Cesar and Grice 2018).

C_{19}–C_{26} cheilanthane TT are the main research objects this time, and their distribution characteristics are shown in Fig. 8. The crude oil in the study area contains relatively

Table 4 The full name of the compound corresponding to each peak in the m/z 191, m/z 123, and m/z 217 chromatograms

Peak	Full name	Peak	Full name	Peak	Abbreviations	Full name
TT	Tricyclic terpane	C_{34}αβ S	17α(H), 21β(H)-C_{34} hopane(22S)	a	C_{27}ααα 20R sterane	5α(H),14α(H),17α(H)-C_{27}sterane(20R)
Ts	18α(H)-C_{27} trisnorhopane	C_{34}αβ R	17α(H),21β(H)-C_{34} hopane(22R)	b	C_{28}ααα 20R sterane	24-Methyl-5α(H),14α(H),17α(H)-C_{28}sterane(20R)
Tm	17α(H)-C_{27} trisnorhopane	1	4,4,8,8,9-Pentamethyldecalin	c	C_{29}ααα 20S sterane	24-Ethyl-5α(H),14α(H),17α(H)-C_{29} sterane(20S)
C_{29}αβ	17α(H), 21β(H)-C_{29} norhopane	2	C_{15}bicyclic sesquiterpanes	d	C_{29}αββ 20R sterane	24-Ethyl-5α(H),14β(H),17β(H)- C_{29} sterane(20R)
C_{30}αβ	17α(H), 21β(H)-C_{30} hopane	3	4,4,8,9,9-Pentamethyldecalin	e	C_{29}αββ 20S sterane	24-Ethyl-5α(H),14β(H),17β(H)- C_{29} sterane(20S)
C_{31}αβ S	17α(H), 21β(H)-C_{31} hopane(22S)	4	C_{15}8β(H)-drimane	f	C_{29}ααα 20R sterane	24-Ethyl-5α(H),14α(H),17α(H)- C_{29} sterane(20R)
C_{31}αβ R	17α(H), 21β(H)-C_{31} hopane(22R)	5	4,4,9,9,10-Pentamethyldecalin			
C_{32}αβ S	17α(H), 21β(H)-C_{32} hopane(22S)	6	C_{16}8α(H)-drimane			
C_{32}αβ R	17α(H), 21β(H)-C_{32} hopane(22R)	7	C_{16}bicyclic sesquiterpanes			
C_{33}αβ S	17α(H), 21β(H)-C_{33} hopane(22S)	8	C_{16}bicyclic sesquiterpanes			
C_{33}αβ R	17α(H), 21β(H)-C_{33} hopane(22R)	9	C_{16}8β(H)-homodrimane			

Table 5 Molecular geochemical data of crude oil and source rocks

Well	Formation	Depth (m)	Terpenes (m/z 191)							Bicyclic sesquiterpene (m/z 123)				Steranes (m/z 217)			m/z 412	Sample
			1	2	3	4	5	6	7	8	9	10	11	12	13	14	15	type
WA1	EP	3391.83	0.16	0.23	0.18	0.34	0.39	2.55	0.92	0.66	0.20	1.09	5.63	0.20	0.41	0.42	3.65	SEP
WA2	EP	3538	0.49	0.33	0.16	0.13	0.38	1.35	0.94	0.78	0.35	1.05	5.35	0.11	0.45	0.43	2.37	
WA3	EP	4507.55	0.58	0.42	0.14	0.30	0.31	1.33	1.63	1.69	0.27	1.02	1.54	0.30	0.41	0.37	3.46	
WA3	EP	4512.15	0.59	0.42	0.16	0.25	0.33	0.74	1.47	1.56	0.28	1.06	1.65	0.63	0.51	0.41	3.17	
WA4	EP	4122	0.65	0.63	0.11	0.40	0.29	3.68	1.35	1.18	0.16	0.62	2.00	0.29	0.46	0.52	0.55	
WA4	EP	4380	0.72	0.62	0.10	0.36	0.28	0.57	1.25	1.35	0.16	0.63	2.34	0.25	0.45	0.57	0.36	
WB1	WC1	3019	0.08	0.25	0.08	0.26	0.37	1.17	1.06	1.01	0.25	1.16	4.99	0.15	0.38	0.39	0.58	SWC
WB1	WC1	3149	0.06	0.25	0.07	0.60	0.40	1.04	0.94	0.87	0.24	1.03	4.81	0.11	0.37	0.38	0.44	
WB1	WC2	3234	0.11	0.72	0.05	0.27	0.38	1.62	0.69	0.51	0.26	1.12	9.35	0.76	0.40	0.54	0.00	MWC
WB1	WC2	3268	0.12	0.73	0.05	0.30	0.37	1.91	0.73	0.61	0.26	1.13	8.50	0.65	0.36	0.58	0.00	
SH1	ZJ1	1269.6	0.16	0.74	0.07	0.41	0.26	2.92	1.60	3.10	0.97	1.35	0.54	0.24	0.34	0.56	0.78	Oil
SH2	ZJ1	1205	0.17	0.76	0.06	0.38	0.29	2.73	1.47	3.38	0.99	1.23	0.53	0.34	0.40	0.54	1.08	
SH3	ZJ1	1224	0.23	0.75	0.06	0.39	0.25	3.24	1.78	2.55	0.85	0.85	0.73	0.29	0.39	0.54	1.10	
SH4	ZJ1	1143.5	0.23	0.77	0.07	0.38	0.30	2.65	1.28	2.02	0.74	0.96	1.07	0.34	0.34	0.57	1.61	
SH4	ZJ1	1144.1	0.29	0.78	0.07	0.44	0.23	4.37	1.84	2.45	0.76	1.02	0.90	0.33	0.39	0.53	1.55	
SH4	ZJ1	1145.8	0.30	0.76	0.05	0.36	0.29	2.74	1.52	3.05	0.79	1.06	0.65	0.28	0.42	0.50	1.59	

1 = ∑TTs/∑Hops = (C_{19}-C_{26}TT)/(C_{29}αβ-C_{34}αβ); 2 = Ts/(Ts + Tm); 3 = Ga/C_{30}H; 4 = (C_{19} + C_{20}TT)/(C_{19}-C_{26}TT); 5 = (C_{21} + C_{23}TT)/(C_{19}-C_{26}TT); 6 = (C_{19} + C_{20}TT)/C_{23}TT; 7 = C_{20}TT/C_{21}TT; 8 = 4,4,8,8,9-pentamethyldecalin/C_{15}8β(H)-drimane; 9 = 4,4,9,9,10-pentamethyldecalin/C_{16}8β(H)-homodrimane; 10 = 4,4,8,9,9-pentamethyldecalin/C_{15}8β(H)-drimane; 11 = C_{16}8β(H)-homodrimane/4,4,8,8,9-pentamethyldecalin; 12 = C_{30}-4MSt/C_{29} Regular sterane; 13 = C_{29}ββ/(ββ + αα); 14 = C_{29}20S/(20S + 20R); 15 = (W + T)/C_{30}Hopane

low cheilanthane tricyclic terpenes, and the ratio of cheilanthane tricyclic terpenes to hopanes (∑TTs/∑Hops) is 0.16 ~ 0.30. The C_{20}TT has the highest content, and it is the main peak carbon. C_{19}–C_{20}–C_{21}–C_{23}TT presents a "low–high-low" distribution characteristic, which means that the C_{19}–C_{20} tricyclic terpenes imported from terrestrial sources are higher than the C_{21}–C_{23} tricyclic terpenes representing lacustrine inputs. The ratio of (C_{19} + C_{20})/(C_{19}–C_{26}) TT is 0.36 ~ 0.44, and the value of (C_{21} + C_{23})/(C_{19}–C_{26}) TT is distributed between 0.23 and 0.30, (C_{19} + C_{20})/(C_{23}) TT is 2.65 ~ 4.37, and the value of C_{20}/C_{21}TT is 1.28–1.84. This indicates that the crude oil from the Shenhu uplift has a larger proportion of its parent source from terrestrial organisms.

The C_{19}–C_{20}–C_{21}–C_{23}TT of MWC also presents a "low–high-low" distribution, but with C_{21}TT as the main peak, and C_{21}–C_{23}TT is higher than C_{19}–C_{20}TT. For example, the value of (C_{19} + C_{20})/(C_{19}–C_{26}) TT is between 0.27 and 0.30, and the value of (C_{21} + C_{23})/(C_{19}–C_{26}) TT is 0.37 ~ 0.38. The C_{19}-C_{20}-C_{21}-C_{23}TT of the SWC are "upward." The tricyclic terpane characteristics of the above two sets of source rocks are quite different from crude oil. In addition, the source rocks of SEP in Wenchang-A depression are inequal in tricyclic terpenes, showing different distribution characteristics. However, the distribution characteristics of tricyclic terpenes in the source rock of well WA4 are consistent with the characteristics of the crude oil in the Shenhu uplift. They are all characterized by C_{20}TT as the main peak carbon, with "low–high-low" distribution characteristics. The value of (C_{19} + C_{20})/(C_{19}–C_{26}) TT is 0.36–0.40, (C_{21} + C_{23})/(C_{19}-C_{26}) TT is 0.28–0.29, which indicates that the terrestrial input contributes more to their parent material sources.

The drimane series of dicyclic sesquiterpene is a class of low-molecular biomarkers with carbon numbers ranging from C_{14} to C_{16}, containing multiple isomers, mainly identified on the m/z 123 mass chromatogram of saturated hydrocarbons (Yang et al. 2012). Among them, 4,4,8,8,9-pentamethyldecalin, 4,4,8,9,9-pentamethyldecalin, and 4,4,9,9,10-pentamethyldecalin are formed by rearrangement of drimane. The 4,4,8,8,9-pentamethyldecalin peaks of the crude oil from the Shenhu uplift are higher, and the peak shape distribution characteristics of the wells WA3 and WA4 are similar to it. The values of 4,4,8,9,9-pentamethyldecalin /C_{15}8β(H) drimane and 4,4,9,9,10-pentamethyldecalin/C_{16}8β(H) homodrimane in the crude oil samples are higher than those of the source rock, but relatively close to those of the WA3 and WA4 wells (Fig. 9).

C_{27}–C_{29} regular steranes and 4-methyl steranes

The relevant parameters are shown in Table 5. The full name of the peak in the mass spectrometer-chromatogram is shown in Table 4.

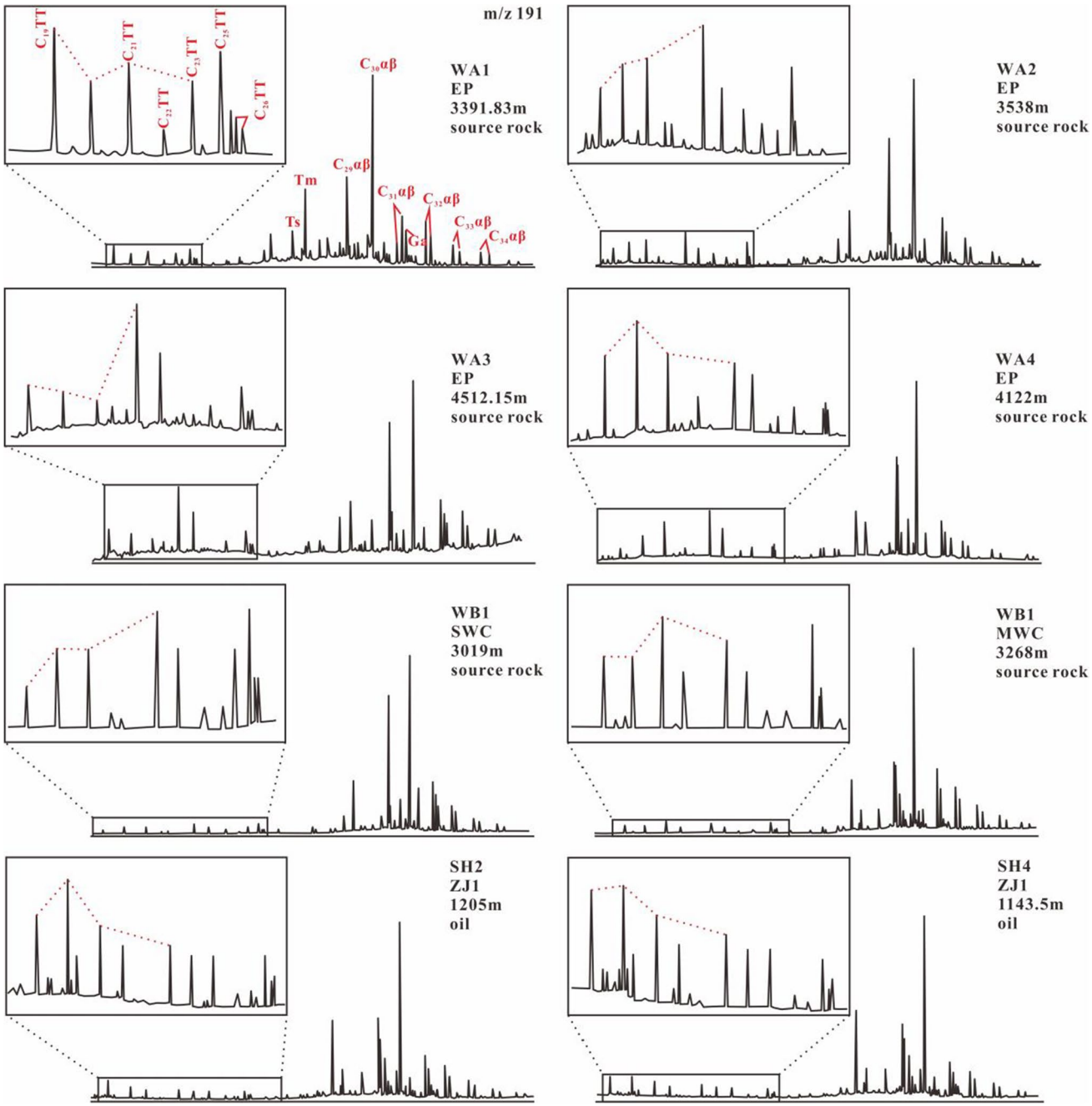

Fig. 8 Terpane mass chromatogram (m/z 191) of crude oil and source rocks

C_{27}–C_{29} regular sterane derived from sterols in eukaryotes and algae (Tissot and Welte 1984). 4-Methyl sterane is a common component of Cenozoic lake sediments in China (Huang et al. 1994). It is dominated mainly in lacustrine environments and has been considered to be associated with abundant algae of dinoflagellates (Wolff et al. 1986) and pavlova gyrans (Volkman et al. 1990) in the PRMB. Therefore, they can be used to analyze the source of the crude oil parent material. It plays an important role in analyzing molecular geochemical characteristics of crude oil and source rocks. The ααα20RC_{27}-ααα20RC_{28}-ααα20RC_{29} regular sterane of crude oil in Shenhu uplift area showed "L" type and has a certain content of C_{30}-4 MSt methyl sterane distribution (Fig. 9). The value of C_{30}-4 MSt/C_{29} regular sterane is between 0.24 and 0.34. As far as the distribution characteristics of steranes are concerned, the characteristics of MWC of Wenchang-B depression are most different from that of crude oil. The ααα20RC_{27}-ααα20RC_{28}-ααα20RC_{29}

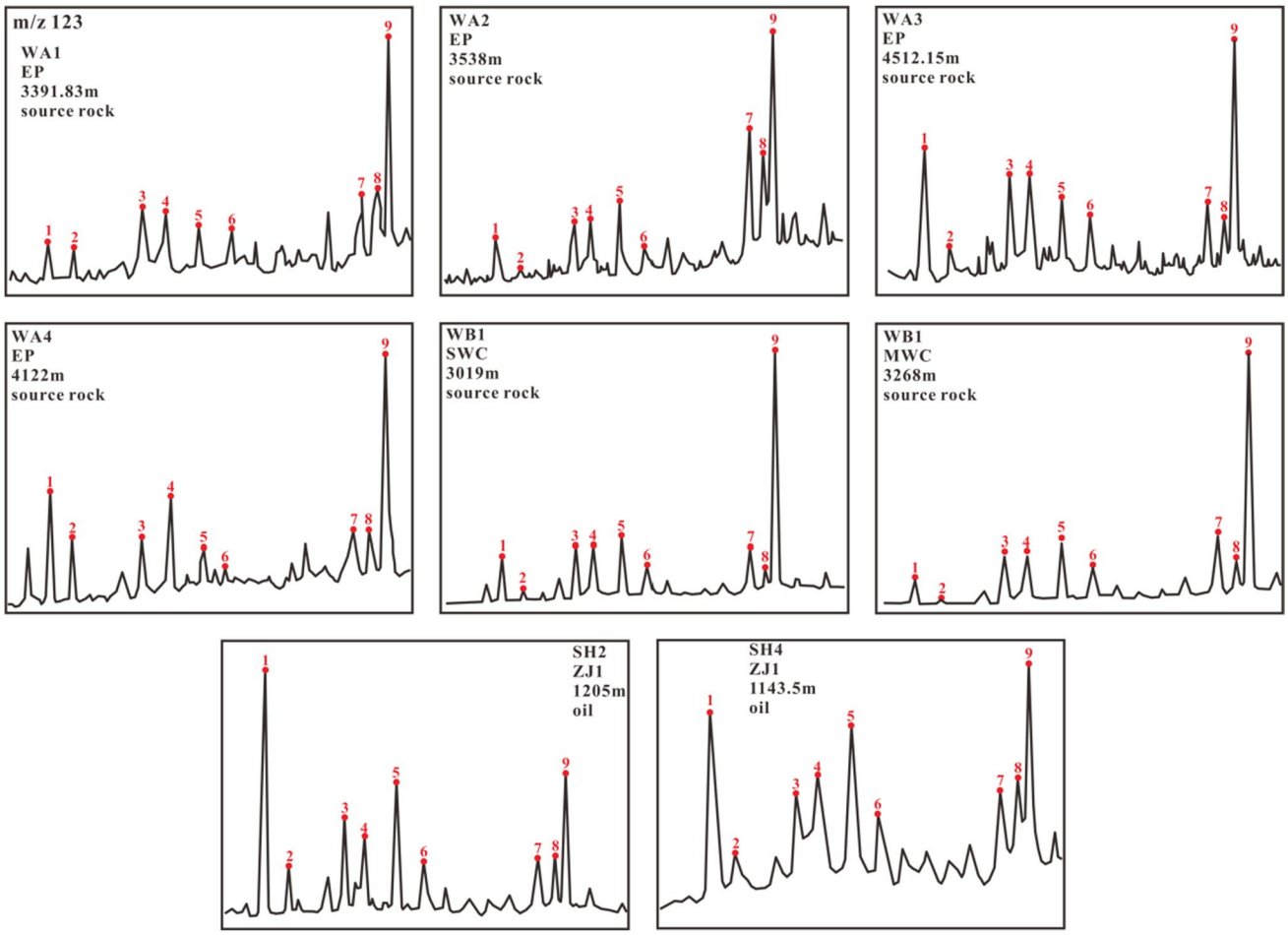

Fig. 9 Bicyclic sesquiterpene mass chromatogram (m/z 123) of crude oil and source rocks

shows a reverse "L" type and contains high C_{30}-4 methyl steranes. The C_{30}-4 MSt/C_{29} regular sterane values are between 0.65 and 0.76, indicating that the relationship between the MWC and crude oil in the study area is weak, and the possibility of crude oil from the source rocks is low. In addition, the regular sterane distribution characteristics of wells WA1, WA3, and WA4 are similar to that of crude oil. WA3 and WA4 wells contain a certain amount of C_{30}-4 methyl sterane, and the C_{30}-4 MSt/C_{29} regular sterane values are 0.30–0.63 and 0.25–0.29, respectively. This indicates that the source of crude oil is more similar to the source rocks of the two wells.

Bicadinanes

Bicadinanes is widely distributed in tertiary sediments and crude oil in Southeast Asia (Zhang et al. 2004). Predecessors have conducted many studies on the characteristics of bicadinanes (Vanaarssen et al. 1990; Yin et al. 2020). It is generally believed that bicadinanes are derived from a resin compound and formed in a partially oxidized depositional environment (Zhu et al. 2006). Due to its unique cracking mode, strong fragmentation peaks can be detected in mass chromatography with various mass-to-charge ratios. In this study, according to the peak position and relative retention time of bicadinanes published in Murray et al (1994), bicadinanes were identified in the m/z 412 mass chromatogram (Fig. 10).

The bicadinanes "W," "T," and peak C_{30}H in the crude oil of the Shenhu uplift area showed a "mountain peak" distribution, with "T" as the main peak, and (W + T)/C_{30}H values ranging from 1.08 to 1.61. Among several sets of source rocks, MWC does not contain bicadinanes, SWC and well WA4 Enping source rock does not contain W, and the (W + T)/C_{30}H value is less than 1.00. Well WA1 and WA2 also have no W peak distribution. Still, the distribution characteristics of bicadinanes in well WA3 are consistent with the crude oil in the study area, and the value of (W + T)/C_{30}H is between 3.17 and 3.46. It shows that the source of crude oil in the study area is mainly higher plants, similar to the characteristics of Well WA3.

Oil source relations

Maturity

The difference between crude oil and source rock has been qualitatively analyzed in 4.2 section, and now the oil-source relationship is quantitatively analyzed in combination with the multi-parameter cross-plot (Fig. 11). Several sterane and terpane isomerization parameters, including C_{29} sterane 20S/ (20S + 20R), C_{29} sterane ββ/ (ββ + αα), Ts/(Ts + Tm), tricyclic/pentacyclic terpanes, as well as Pr/nC_{17} and Ph/nC_{18} ratios have been used widely for maturity evaluation (Gao et al. 2015). On the intersection diagram of C_{29} sterane 20S/(20S + 20R) and C_{29} sterane ββ/(ββ + αα) (Fig. 11a), the source rock in the study area is in the mature interval. The SWC of well WB1 and the SEP of wells WA2 and WA3 are of relatively low maturity, which is somewhat different from the distribution characteristics of crude oil in the Shenhu uplift (Fig. 11 a, b, and c). The source rocks of these three wells may contribute to a certain degree of crude oil accumulation in the Shenhu uplift area. The MWC in well WB1 and the SEP in well WA4 have high maturity. The relevant parameters are consistent with the distribution characteristics of crude oil (Fig. 11 a, b and c), indicating that they are closely related.

Fig. 11 Oil source correlation parameter cross plot (base image from Gao et al. 2015)

Sedimentary environment

The intersection of Pr/nC_{17}-Ph/nC_{18} and Pr/Ph-Gammacerane Index (Ga/C_{30}H) has been used to represent the depositional environment (Gao et al. 2015; Quan et al. 2015), and bicyclic sesquiterpenes also have the meaning of indicating the sedimentary environment (Cesar and Grice 2018). The parameter distribution range of wells WA1 and WA2 is quite different from that of crude oil (Fig. 11 c, d, e, and f), indicating that the water bodies were deposited in different environments at that time. Thus, the possibility that the crude oil came from the source rock of well WA1 and WA2 was ruled out. Judging from the distribution characteristics of bicyclic sesquiterpenes (Fig. 11 e and f), the two sets of source rocks of Wenchang Formation in Wenchang-B depression are quite different from the characteristics of crude oil from the Shenhu uplift, reducing the possibility of crude oil came from these two sets of source rocks. The source rock characteristics of wells WA3 and WA4 are similar to those of crude oil (Fig. 11 c, d, e, and f) and are closely related.

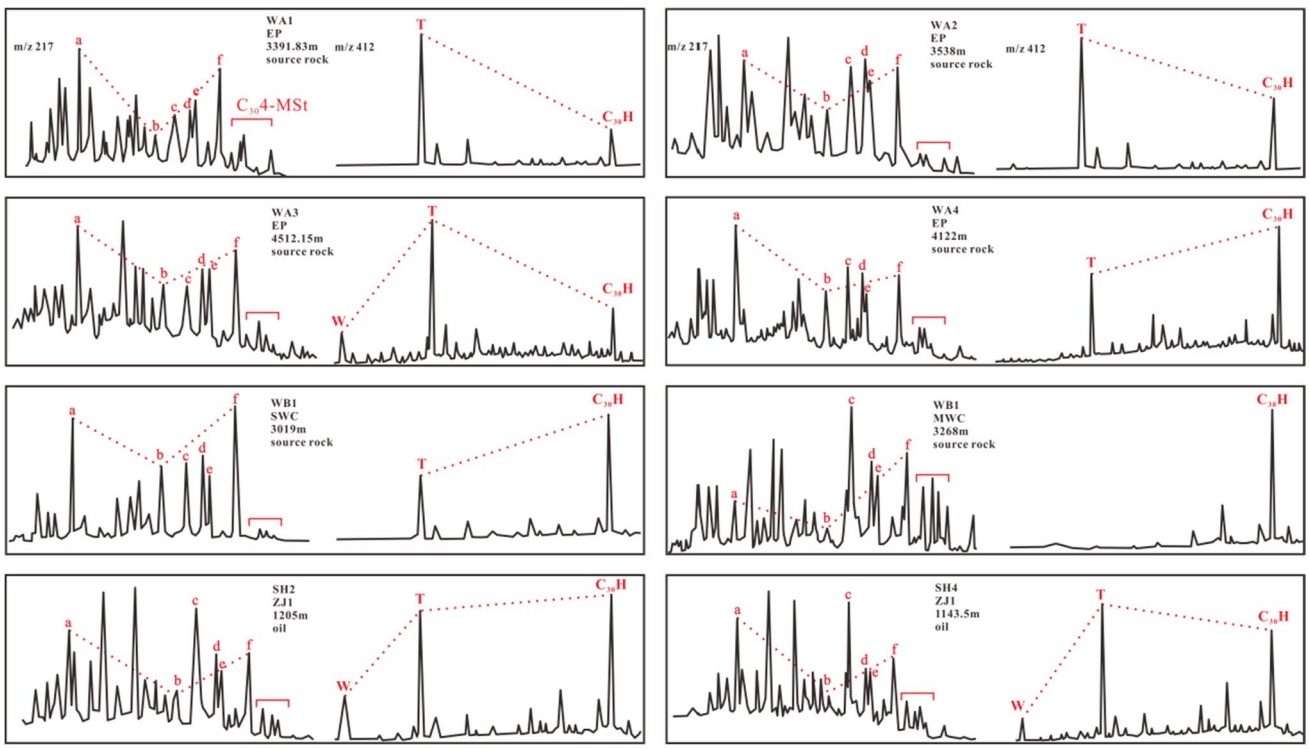

Fig. 10 Mass chromatography (m/z 217 and m/z 412) of crude oil and source rocks

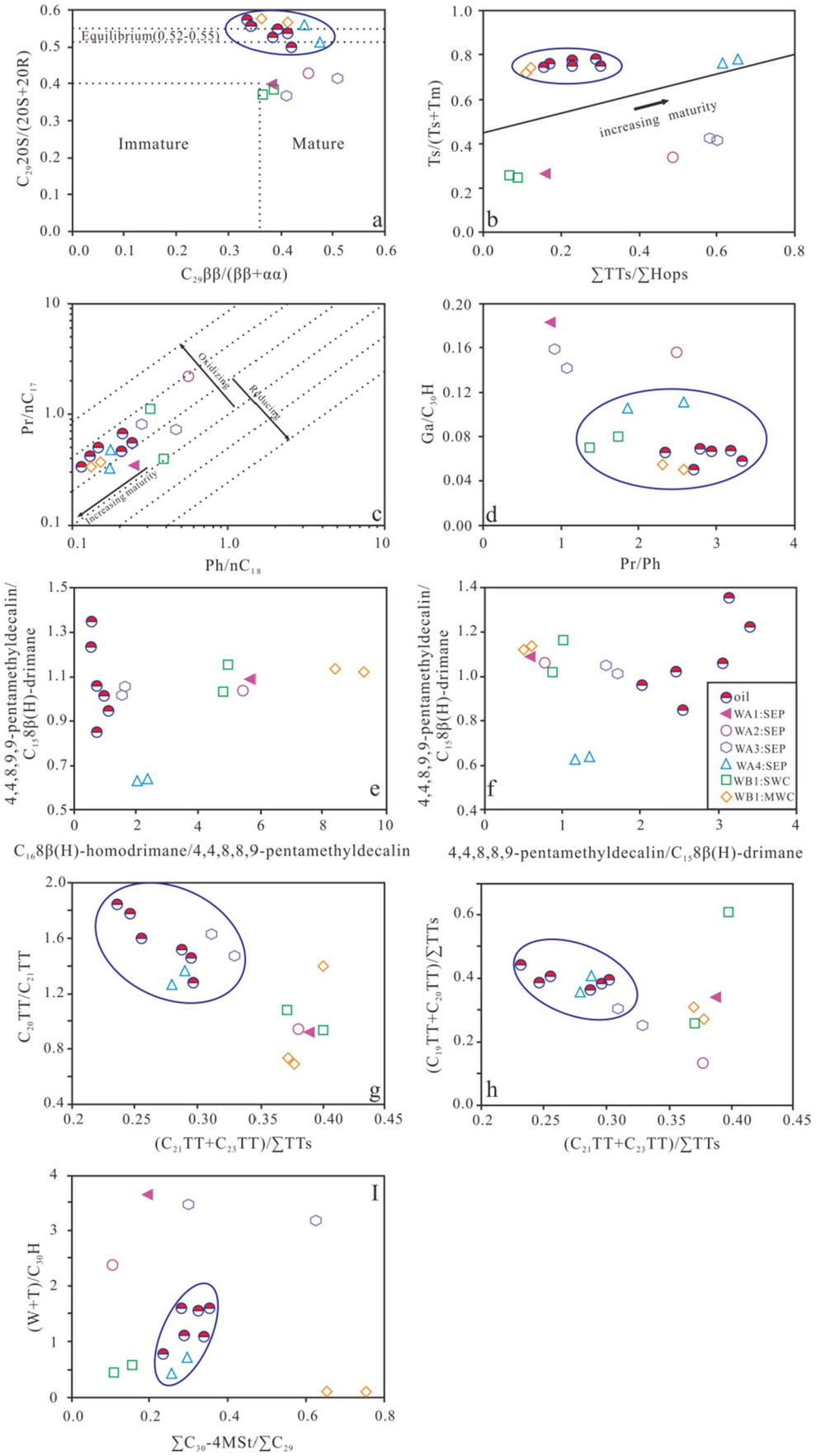
Equilibrium(0.52-0.55)
Immature
Mature
C29 20S/(20S+20R)
C29ββ/(ββ+αα)
a
Ts/(Ts+Tm)
increasing maturity
∑TTs/∑Hops
b
Pr/nC17
Ph/nC18
Oxidizing
Reducing
Increasing maturity
c
Ga/C30H
Pr/Ph
d
4,4,8,9,9-pentamethyldecalin/C15 8β(H)-drimane
C16 8β(H)-homodrimane/4,4,8,8,9-pentamethyldecalin
e
4,4,8,8,9-pentamethyldecalin/C15 8β(H)-drimane
oil
WA1:SEP
WA2:SEP
WA3:SEP
WA4:SEP
WB1:SWC
WB1:MWC
f
C20TT/C21TT
(C21TT+C23TT)/∑TTs
g
(C19TT+C20TT)/∑TTs
(C21TT+C23TT)/∑TTs
h
(W+T)/C30H
∑C30-4MSt/∑C29
I

Parent material

The related parameters of tricyclic terpenes reflect the parent source relationship of crude oil in the study area. C_{30}-4 methyl sterane has been widely used in studying the source of parent material in the Zhu-3 depression (Volkman et al. 1990; Tao et al. 2015). Figure 11 g shows that the crude oil and the two sets of source rocks in the Wenchang-B depression are quite different. The relevant parameters are distributed in different intervals. Therefore, the possibility that the crude oil came from the source rocks of the Wenchang Formation in the Wenchang-B depression can be ruled out. It can be seen from Fig. 1 that both wells WA3 and WA4 are close to the deposition center of Wenchang-A depression, and their other characteristics are similar. To further explore the differences between the two and their relationship with crude oil. Draw the intersection diagram of C_{30}-4MSt/C_{30}H and (W + T)/C_{30}H (Fig. 11i). It is found that the parameters of crude oil are consistent with the distribution of well WA4 and are different from well WA3. It shows that the parent source of wells WA3 and WA4 is different, and the parent material source of crude oil is the same as that of well WA4.

Source of crude oil

Quan et al (2015) believed that the crude oil came from the Wenchang-B depression (Fig. 12). However, this understanding is relatively shallow and does not consider more geological conditions. First of all, the geological conditions of Wenchang-B depression are complicated, and there is no more systematic study on the activity and sealing of faults. Secondly, the oil generated in Wenchang-B depression needs to pass through Wenchang-C depression to migrate to the Shenhu uplift. The geological conditions of Wenchang-C depression are less understood at this stage. Last but not least, through the previous analysis from the article, the geochemical characteristics have ruled out the possibility that the crude oil in the Shenhu uplift area came from the Wenchang-B depression. Therefore, this study believes that the accumulation of crude oil in the Shenhu uplift area should be as shown in Figure 13: the crude oil came from the shallow lacustrine source rock of the Enping Formation in well WA4 and migrated vertically through the fault to the Zhujiang Formation. Laterally, the sand bodies migrated along the steep slope to form reservoirs in the study area.

Conclusions

1. There are mainly three sets of source rocks in the Zhu-3 sub-basin: MWC and SWC source rocks in Wenchang-B depression, and SEP source rocks in Wenchang-A depression. The three sets of source rocks have a good hydrocarbon generation potential, and the MWC is the best. In order to refine the characteristics of the source rock in Wenchang-A depression, four wells with different distances from the

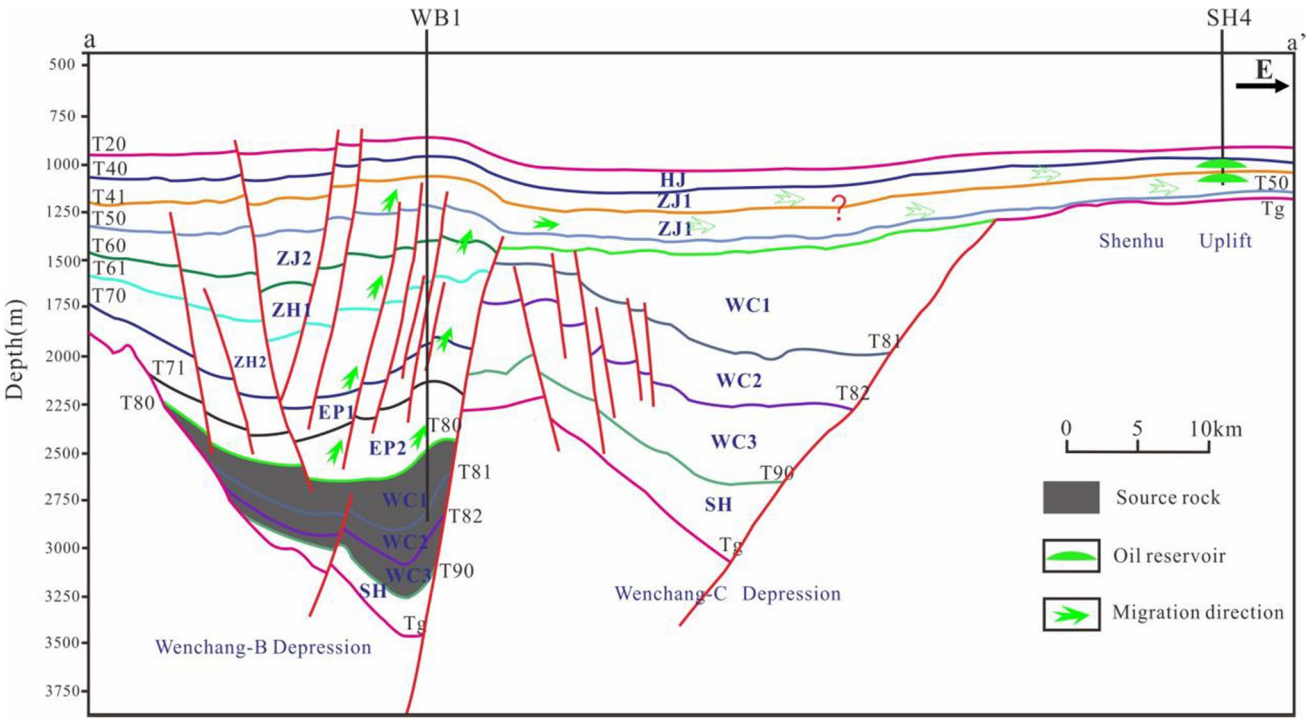

Fig. 12 Geological profile of Wenchang-B depression–Shenhu uplift area (a–a')

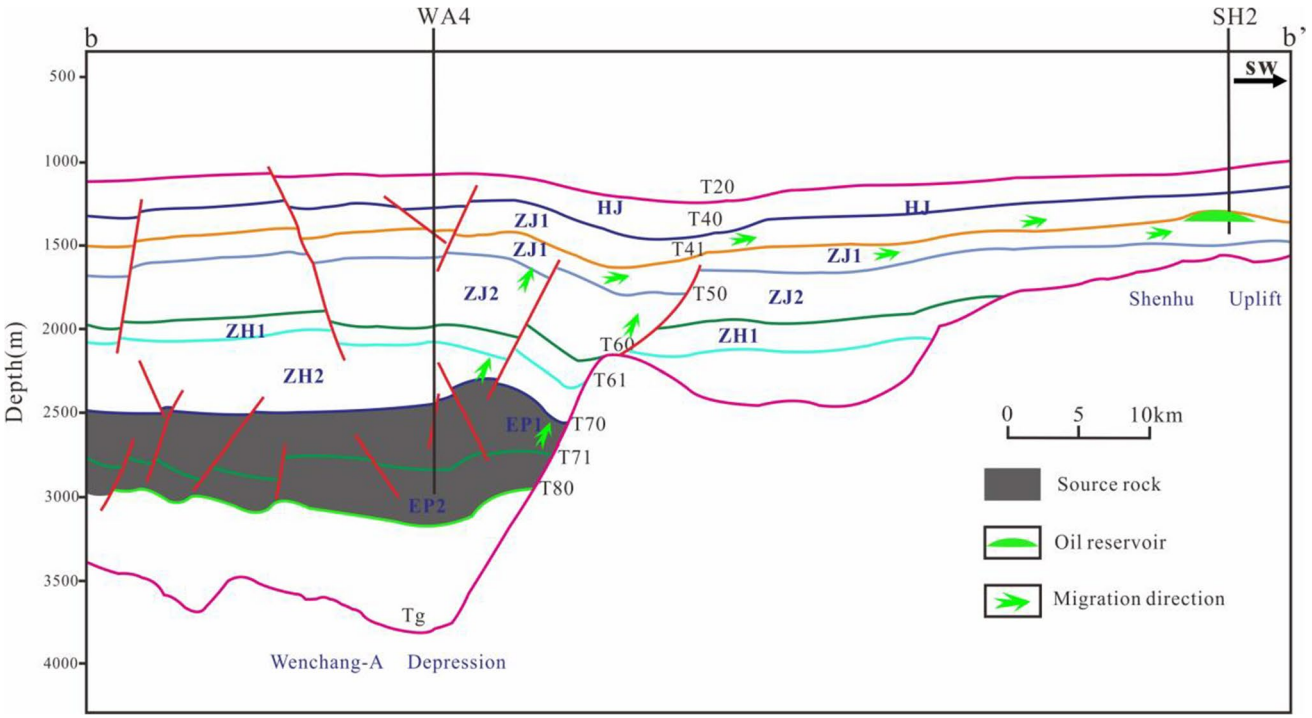

Fig. 13 Geological profile of Wenchang-A depression–Shenhu uplift area (b–b')

deposition center were selected. The well WA1 far from the deposition center has low maturity and low hydrocarbon generation potential.

2. Using multiple parameters to determine the characteristics and source of crude oil, and comparing the difference between crude oil and the source rock of each well one by one, it was found that (i) in terms of sedimentary environment characteristics, the difference between crude oil and the source rock of wells WA1 and WA2 is the biggest, followed by the two sets of source rocks of the Wenchang Formation in Wenchang-B depression; (ii) the source of crude oil parent material is the closest to the source rock of well WA4.

3. Through the above analysis, combined with the geological profile, the possibility of crude oil accumulation combined with the characteristics of crude oil accumulation is analyzed. It is believed that the crude oil came from well WA4, which is the nearest to the center of Wenchang-A depression. It migrated upwards through faults in the vertical direction, and then migrated along the steep slope belt to the Shenhu uplift to form reservoirs. In the future, more relevant studies can be conducted on faults and the direction of oil and gas migration, and this possibility may be proved from experiments and data analyses.

Acknowledgements Funding for this research was provided by the development mechanism of high-quality source rocks and hydrocarbon accumulation regularity in Zhusan depression (NO. CCL2020ZJFN0226) and National Natural Science Foundation of China: Study on the Control Mechanism of the Formation of Terrestrial Tight Oil (Low Permeability Reservoir) by the Mud/Calcium Interval between Source and Reservoir (NO.41872165). Appreciation is expressed to the Hainan Branch of China National Offshore Oil Corporation Ltd, predecessors for all of their previous researches and AG for providing a platform to publish my paper, and thank editors and reviewers for taking their time to review this paper.

Author contribution Xiaoyan Fu: conceptualization, methodology, writing, and editing. Junjun You and Shijia Chen: guidance, review. Xin He: drawing. Hui Li and Mingzhu Lei: supervision, project administration, and funding acquisition. All of the authors have read and agreed to the published version of the manuscript.

Declarations

Conflict of interest The authors declare that they have no competing interests.

References

Aichner B, Herzschuk U, Wilkes H (2010) Influence of aquatic macrophytes on the stable carbon isotopic signature of sedimentary organic matter in lakes on the Tibetan Plateau. Org Geochem 41:706–718. https://doi.org/10.1016/j.orggeochem.2010.02.002

Ahmed OE, El Fadly AA, El Nady MM (2017) Evaluation of biogenic and anthropogenic inputs sediment along the Suez Gulf Shoreline: an implication from aliphatic and alicyclic hydrocarbons. Energy Sources A: Recovery, Util Environ Eff

39(4):389–397. https://doi.org/10.1080/15567036.2016.1217294

Aldahik AH, Schulz M, Horsfield B, Wilkes H, Dominik W, Nederlof P (2017) Crude oil families in the euphrates graben (Syria). Mar Pet Geol 86:325–342. https://doi.org/10.1016/j.marpetgeo.2017.05.030

Ahmed A, Khan T, Jahandad S, Hakimi MH, Lashin AA, Abidin NSZ (2020) Organic geochemistry indicates source-rock characteristics and hydrocarbon potential: A case study from Early Cretaceous Sembar Formation, southern Indus Basin, Pakistan. Arab J Geosci. 13:1234. https://doi.org/10.1007/s12517-020-06227-4

Brooks J, Thusu B (1977) Oil-source rock identification and characterization of the Jurassic sediments in the northern North Sea. Chem Geol 20:283–294. https://doi.org/10.1016/0009-2541(77)90053-5

Bechtel A, Oberauer K, Kostic A, Gratzer R, Milisavljevic V, Aleksic N, Stojanovic K, Grob D, Sachsenhofer RF (2018) Depositional environment and hydrocarbon source potential of the Lower Miocene oil shale deposit in the Aleksinac Basin (Serbia). Org Geochem 115:93–112. https://doi.org/10.1016/j.orggeochem.2017.10.009

Biswas S, Varma AK, Kumar M, Mani D, Saxena VK, Mishra V (2020) Influence of geochemical, organo-petrographically and palynofacies assemblages on hydrocarbon generation: a study from upper Oligocene coal and shale of the Makum Coal Basin, Assam, India. Mar Pet Geol. 114:104206. https://doi.org/10.1016/j.marpetgeo.2019.104206

Cao QY (1985) Identification of micro-components and types of kerogen under transmitted light. Petroleum exploration and development. 05:14–23+81–88.

Cox HC, Deleeuw JW, Schenck PA et al (1986) Bicadinane, a C_{30} pentacyclic isoprenoid hydrocarbon found in crude oil. Nature 319(6051):316–318. https://doi.org/10.1038/319316a0

Chen SP, Liu LF, Huang SB (2015) Study on petroleum accumulation patterns in WC15-1 structure in Shenhu uplift. Special Reservoir. 22(4):14-17. 10.3969/ j. issn.1006-6535.2015.03.003. (In Chinese with English abstract)

Cheng P, Xiao XM, Gai HF, Li TF, Zhang YZ, Huang BJ, Wilkins RWT (2015) Characteristics and origin of carbon isotopes of n-alkanes in crude oils from the western Pearl River Mouth Basin, South China sea. Mar Pet Geol 67:217–229. https://doi.org/10.1016/j.marpetgeo.2015.05.0280

Cesar J, Grice K (2018) Drimane-type compounds in source rocks and fluids from fluvial-deltaic depositional settings in the North-West Shelf of Australia. Org Geochem 116:103–112. https://doi.org/10.1016/j.orggeochem.2017.11.012

Elias VO, Simoneit BR, Cardoso JN (1997) Even n-alkane predominance on the Amazon shelf and a Northeast Pacific hydrothermal system. Naturwissenschaften 84:415–420. https://doi.org/10.1007/s001140050421

El-Nemr A, Moneer AA, Ragab S, El-Sikaily A (2016) Distribution and sources of n-alkanes and polycyclic aromatic hydrocarbons in shellfish of the Egyptian Red Sea coast. Egypt J Aquat Res 42:121–131. https://doi.org/10.1016/j.ejar.2016.05.003

Fu N, Li YC, Sun JX, Sun YM, Xu JY (2011) Recognition of Oil Source and Source Rocks in Zhu III Depression. Geoscience. 25(06):1121-1130. https://doi.org/10.3969/j.issn.1000-8527.2011.06.010. (In Chinese with English abstract)

Ficken KJ, Li B, Swain DL, Wglinton G (2000) An n-alkane proxy for the sedimentary input of submerged/floating freshwater aquatic macrophytes. Org Geochem 31:745–749. https://doi.org/10.1016/S0146-6380(00)00081-4

Grande SMBD, Neto FRA, Mello MR (1993) Extended tricyclic terpanes in sediments and petroleums. Org Geochem 20(7):1039–1047. https://doi.org/10.1016/0146-6380(93)90112-O

Gao P, Liu GD, Jia CZ, Ding XJ, Chen ZL, Dong YM, Zhao X, Jiao WW (2015) Evaluating rare earth elements as a proxy for oil–source correlation. A case study from Aer Sag, Erlian Basin, northern China. Org Geochem 87:35–54. https://doi.org/10.1016/j.orggeochem.2015.07.004

Hunt J (1979) Petroleum Geochemistry and Geology. Freeman W. H., San Francisco

Huang DF, Zhang DJ, Li JC (1994) The origin of 4-methyl steranes and pregnanes from Tertiary strata in the Qaidam Basin China. Org Geochem 22(2):343–348. https://doi.org/10.1016/0146-6380(94)90180-5

Huang BJ, Xiao XM, Zhang MQ (2003) Characteristics and origin of carbon isotopes of n-alkanes in crude oils from the western Pearl River Mouth Basin, South China sea. Org Geochem. 34(7):993–1008. https://doi.org/10.1016/S0146-6380(03)00035-4

Huang BJ, Xiao XM, Cai DS, Wilkins RWT, Liu MQ (2011) Oil families and their source rocks in the Weixinan sub-basin, Beibuwan basin, south China sea. Org Geochem 42(2):134–145. https://doi.org/10.1016/j.orggeochem.2010.12.001

Hao F, Zhou XH, Zhu YM, Yang YY (2011) Lacustrine source rock deposition in response to co-evolution of environments and organisms controlled by tectonic subsidence and climate, Bohai Bay Basin, China. Org Geochem 42(4):323–339. https://doi.org/10.1016/j.orggeochem.2011.01.010

Hakimi MH, Abdullah WH, Sia SG, Makeen YM (2013) Organic geochemical and petrographic characteristics of Tertiary coals in the northwest Sarawak, Malaysia: Implications for palaeoenvironmental conditions and hydrocarbon generation potential. Mar Pet Geol 48:31–46. https://doi.org/10.1016/j.marpetgeo.2013.07.009

Hu Y, Hao F, Zhu JZ, Tian JQ, Ji YB (2014) Origin and occurrence of crude oils in the Zhu1 sub-basin Pearl River Mouth Basin China. J Asian Earth Sci 97(2015):24–37. https://doi.org/10.1016/j.jseaes.2014.09.041

Jiang H, Wang H, Li JL, Chen SP, Lin ZL, Fang XX, Cai J (2009) Research on hydrocarbon pooling and distribution patterns in the Zhu-3 Depression, the Pearl River Mouth Basin. Oil Gas Geology. 30(03):275–281+286. (In Chinese with English abstract)

Kang K, Feng M (2011) The study of geochemistry characteristics of the oil of Wenchang 13-1/2 oilfields. Offshore Oil. 31(01):48-52. doi:1008-2336 (2011) 01-0048-05. (In Chinese with English abstract)

Lin XR, Sun ZP (1999) Conditions of forming gas reservoirs in Wenchang sag A. Gas Ind. 19(1):52-57. (In Chinese with English abstract)

Luo ZY, Lu JG, Zou HL, Li YP, Hu ZZ (2020) Influence of methane diffusion on geochemical characteristics of natural gas: a case study of the Shiqiantan area in Junggar Basin, China. Energy Sources, Part A: Recovery, Utilization, and Environmental Effects. https://doi.org/10.1080/15567036.2020.1812771

Mackenzie AS (1984) Applications of biological markers in petroleum geochemistry. Adv Pet Geochem 01:115–206. https://doi.org/10.1016/B978-0-12-032001-1.50008-0

Murray AP, Padley D, Mckirdy DM, Booth WE, Summons RE (1994) Oceanic transport of fossil dammar resin: the chemistry of coastal resinites from South Australia. Geochim Cosmochim Acta 58(14):3049–3059. https://doi.org/10.1016/0016-7037(94)90178-3

Mayers PA, Ishiwatari R (1995) Organic matter accumulation records in lake sediments. In: Lerman A, Imboden DM, Gat JR (eds) Physics and Chemistry of Lakes. Springer, Berlin, 279–328. https://doi.org/10.1007/978-3-642-85132-2_10

Neto FRA, Restle A, Connan J, Albrecht P (1982) Ourisson G (1982) Novel tricyclic terpanes (C19, C20) in sediments and petroleums. Tetrahedron Lett 23(19):2027–2030. https://doi.org/10.1016/S0040-4039(00)87251-2

Ourisson G, Albrecht P, Rohmer M (1982) Predictive microbial biochemistry — from molecular fossils to procaryotic membranes. Trends Biochem Sci 7(7):236–239. https://doi.org/10.1016/0968-0004(82)90028-7

Ortiz JE, Diaz- Bautista A, Aldasoro JJ, Torres T, Gallego JLR, Moreno L, Estebanez B (2011) N Alkan 2-ones in peat- forming plants from the Ronanzas ombrotrophic bog (Asturias, northern Spain). Org Geochem 42:586–592

Peters KE, Moldowan JM (1994) The biomarker guide: interpreting molecular fossils in petroleum and ancient sediments. Prentics Hall, Englewood Cliffs, New jersey

Punyu VR, Hariji RR, Bhosle NB, Sawant K (2013) n-Alkanes in surficial sediments of Visakhapatnam harbor, east coast of India. J Earth Syst Sci 122(2):467–477. https://doi.org/10.1007/s12040-013-0268-0

Patra S, Dirghangi SS, Rudra A, Dutta S, Ghosh S, Varma AK, Shome D, Kalpana MS (2018) Effects of thermal maturity on biomarker distributions in Gondwana coals from the Satpura and Damodar Valley Basins, India. Int J Coal Geol 196:63–81. https://doi.org/10.1016/j.coal.2018.07.002

Quan YB, Liu JZ, Zhao DJ, Hao F, Wang ZF, Tian JQ (2015) The origin and distribution of crude oil in Zhu III sub-basin, Pearl River Mouth Basin, China. Mar Pet Geol. 66(4):732–747. https://doi.org/10.1016/j.marpetgeo.2015.07.015

Rubinstein I, Spyckerelle C, Strausz OP (1979) Pyrolysis of asphaltenes: a source of geochemical information. Geochim Cosmochim Acta 43(1):1–6. https://doi.org/10.1016/0016-7037(79)90041-3

Resmi P, Manju MN, Gireeshkumar TR, Ratheesh Kumar CS, Chandramohanakumar N (2016) Source characterisation of Sedimentary organic matter in mangrove ecosystems of northern Kerala, India: inferences from bulk characterization and hydrocarbon biomarkers. Reg Stud Mar Sci 7:43–54. https://doi.org/10.1016/j.rsma.2016.05.006

Seifert W, Moldowan J (1978) Applications of steranes, terpanes and monoaromatics to the maturation, migration and source of crude oils. Geochem Cosmochim Acta 42:77–95. https://doi.org/10.1016/0016-7037(78)90219-3

Simoneit BRT, Leif RN, Neto FRA, Azevedo DA, Pinto AC, Albrecht P (1990) On the presence of tricyclic terpane hydrocarbons in permian tasmanite algae. Naturwissenschaften 77(8):380–383. https://doi.org/10.1007/BF01135736

Schwark L, Frimmel A (2004) Chemostratigraphy of the Posidonia Black Shale, SW-Germany: II. Assessment of extent and persistence of photic-zone anoxia using aryl isoprenoid distributions. Chem Geol 206:231–248. https://doi.org/10.1016/j.chemgeo.2003.12.008

Stout SA, Uhler AD, Mccarthy KJ (2005) Middle distillate fuel fingerprinting using drimane-bases bicyclic sesquiterpanes. Environ Forensics 6(3):241–251. https://doi.org/10.1080/15275920500194407

Samuel OJ, Kildahl-Andersen G, Nytoft HP, Johansen JE, Jones M (2010) Novel tricyclic and tetracyclic terpanes in Tertiary deltaic oils: Structural identification, origin and application to petroleum correlation. Org Geochem 41(12):1326–1337. https://doi.org/10.1016/j.orggeochem.2010.10.002

Samad SK, Mishra DK, Mathews RP, Ghosh S, Mendhe VA, Varma AK (2020) Geochemical attributes for source rock and palaeoclimatic reconstruction of the Auranga Basin, India. J Petrol Sci Eng 185:106665. https://doi.org/10.1016/j.petrol.2019.106665

Su KM, Chen SJ, Hou YT, Zhang HF, Zhang WX, Liu GL, Hu C, Han MM (2021) Geochemical characteristics, origin of the Chang 8 oil and natural gas in the southwestern Ordos Basin, China. J Petrol Sci Eng 200(2021):108406. https://doi.org/10.1016/j.petrol.2021.108406

Tissot BP, Welte DH (1978) Petroleum formation and occurrence, Springer-Verlog, Berlin Heidelberg, New York

Tissot BP, Welte DG (1984) Petroleum formation and occurrence, 2nd edn. Springer-Verlag, Berlin, p 699

Tao SZ, Wang CY, Du JG, Liu L, Chen Z (2015) Geochemical application of tricyclic and tetracyclic terpanes biomarkers in crude oils of NW China. Mar Pet Geol 67(6):460–467. https://doi.org/10.1016/j.marpetgeo.2015.05.030

Tewari A, Dutta S, Sarkar T (2017) Biomarker signatures of Permian Gondwana coals from India and their palaeobotanic significance. Palaeogeogr Palaeoclimatol Palaeoecol 468:414–426. https://doi.org/10.1016/j.palaeo.2016.12.014

Tiwari B, Ojha A, Ghosh S, Varma KV, Mendhe VA, Mondal A (2020) A composite microstructural and geochemical approach to quench the quest for hydrocarbon from Barren Measures shales of Jharia Basin, India. J Nat Gas Sci Eng 78:103310. https://doi.org/10.1016/j.jngse.2020.103310

Vanaarssen B, Kruk C, Hessels J, Deleeuw J (1990) Cis-cis-trans-bicadinane, a novel member of an uncommon triterpane family isolated from crude oils. Tetrahedron Lett 31(32):4645–4648. https://doi.org/10.1016/S0040-4039(00)97697-4

Volkman JK, Kearney P, Jeffrey SW (1990) A new source of 4-methy sterols and 5- alpha(H)- stanols in sediments – prymnesiophyte microalgae of the genus pavlova. Org Geochem 15(5):489–497. https://doi.org/10.1016/0146-6380(90)90094-G

Varma AK, Biswas S, Patil JD, Mani D, Misra S, Hazra B (2019) Significance of lithotypes for hydrocarbon generation and storage. Fuel 235:396–405. https://doi.org/10.1016/j.fuel.2018.07.111

Wu CL (1984) Nan Hai (the South China Sea) movement and development of basins in the South China Sea. Mar Sci Bull 3:2 (In Chinese with English abstract)

Wolff GA, Lamb NA, Maxwell JR (1986) The origin and fate of 4-methyl steroid hydrocarbons. 1. diagenesis of 4-methyl sterenes. Geochim Cosmochim Acta 50(3):335–342. https://doi.org/10.1016/0016-7037(86)90187-0

Wu SG, Gao JW, Zhao SJ, Lvdmann T, Chen DX, Spence G (2014) Post-rift uplift and focused fluid flow in the passive margin of northern South China Sea. Tectonophysics. 615–616:27–39. https://doi.org/10.1016/j.tecto.2013.12.013

Wang JY, Guo SB (2020) Comparison of geochemical characteristics of marine facies, marine-continental transitional facies and continental facies shale in typical areas of China and their control over organic-rich shale. Energy Sources, Part A: Recovery, Utilization, and Environmental Effects. https://doi.org/10.1080/15567036.2020.1796855

Xia KY, Huang CL, Jiang SR, Zhang YX, Su DQ, Xia SG, Chen ZR (1994) Comparison of the tectonics and geophysics of the major structural belts between the northern and southern continental margins of the South China Sea. Tectonophysics 235(1–2):99–116. https://doi.org/10.1016/0040-1951(94)90019-1

Xu XD, Huang BJ (2000) A Study on the migration and accumulation of oil and gas in Qionghai ulift, Zhusan depression. Petroleum Exploration and Development 27(4): 41–44+111–120. (In Chinese with English abstract)

Xiao XM, Li NX, Gan HJ, Jin YB, Tian H, Huang BJ, Tang YC (2009) Tracing of deeply-buried source rock: A case study of the WC9-2 petroleum pool in the Pearl River Mouth Basin, South China Sea. Mar Pet Geol 26(8):1365–1378. https://doi.org/10.1016/j.marpetgeo.2009.02.009

Xie RY, Huang BJ, You JJ, Wang BW, Wang LF (2012) The geochemical characteristics and hydrocarbon generation potential of the high-quality source rock in Wenchang sag. China Min. Mag. 21(09):69–71+75. (In Chinese with English abstract)

Xiao ZL, Chen SJ, Li Y, Su KM, He QB, Han MM (2021) Local high-salinity source rock and origin of crude oil in the xianshuiquan structure in the northwestern Qaidam Basin, China. J Petrol Sci Eng 198:108233. https://doi.org/10.1016/j.petrol.2020.108233

Yang BJ, Zheng L, Zhang KY, Chen JH, Wang XR (2012) Oil fingerprint analysis of bicyclic sesquiterpanes by internal standard method and oil identification. Fenxi Ceshi Xuebao: Journal of Instru▪mental Analysis. 31(11):1421–1425. doi:10. 3969 /j. issn.1004–4957. 2012. 11. 014

Yin M, Huang HP, Brown M et al (2020) A novel biodegradation parameter derived from bicyclic sesquiterpanes for assessing moderate levels of petroleum biodegradation. Org Geochem 147:104049. https://doi.org/10.1016/j.orggeochem.2020.104049

Zhu WL, Li MB, Duan PQ, Wang PX, Wu GX, Zhao QH (1997) Palaeolimnology and hydrocarbon potential in Zhu III sub-basin, Pear River Mouth Basin. China Offshore Oil Gas 01:13–18

Zhu WL, Li MB, Wu PK (1999) Petroleum systems of the Zhu III sub-basin, Pearl River Mouth Basin, South China Sea. AAPG Bulletin. 83(6):990-1003. https://doi.org/10.1306/E4FD2E47-1732-11D7-8645000102C1865D

Zhou WW, Zhang HL (2000) Study on application of organic inclusions in Zhu III depression. Acta Petrologica Sinica 16(4):677–686

Zhang SC, Gong ZS, Liang D et al (2004) Geochemistry of petroleum systems in the eastern Pearl RiverMouth Basin-I: oil family classification, oil-source correlationand mixed oil analysis. Acta Sedimentol Sin 22(S1):15–26. https://doi.org/10.3969/j.issn.1000-0550.2004.z1.003.(InChinesewithEnglishabstract)

Zhu JZ, Shi HS, Pang X et al (2006) Geochemical characteristics and oil sources of condensates in Panyu Low Uplift, Pearl River Mouth basin. China Offshore Oil and Gas 18(2):103–106 (In Chinese with English abstract)